Aggregative Effects of Humic Materials in Aqueous Solution

A Dissertation

Presented in Partial Fulfillment of the Requirements for the

Degree of Doctorate of Philosophy

with a

Major in Chemistry

in the

College of Graduate Studies

University of Idaho

by

Leah M. Shaffer

Major Professor: Ray von Wandruszka, Ph.D.

Committee Members: Kris Waynant, Ph.D.; Francis Cheng, Ph.D.; Robert Heinse, Ph.D.

Department Administrator: Ray von Wandruszka, Ph.D.

July 2015

Authorization to Submit Dissertation

This dissertation of Leah M. Shaffer, submitted for the degree of doctorate of philosophy with a Major in chemistry and titled "Aggregative Effects of Humic Materials in Aqueous Solution," has been reviewed in final form. Permission, as indicated by the signatures and dates below, is now granted to submit final copies to the College of Graduate Studies for approval.

Major Professor: _____ Date: _____
Ray von Wandruszka, Ph.D.

Committee Members: _____ Date: _____
Kris Waynant, Ph.D.

_____ Date: _____
Francis Cheng, Ph.D.

_____ Date: _____
Robert Heinse, Ph.D.

Department Administrator: _____ Date: _____
Ray von Wandruszka, Ph.D.

Abstract

The importance of the aggregative effects of humic polymers in soil systems has been well documented. The work described here was undertaken to further elucidate the aggregation of humates with an eye on both analysis and environmental gain. A quinone rich humic material was investigated to clarify the fluorescent effects that result from the conformational changes due to aggregation. Changes to the conformation of humic structure were found to lead to a sequestration of the quinone moieties that lie therein and enhance the fluorescence of these groups by separating them from the aqueous environment that quenches them. This resulted from ionic crosslinking between the carboxylic groups that are abundant in humic materials. The effect is environmentally relevant in view to the ability of humic materials to transport mineral cations through the soil. This investigation dealt with the effect of temperature on the aggregation process. It was shown that aggregation can be induced by raising the temperature of a humate solution that was "primed" by either lowering the pH or the addition of a divalent cations. An increase in temperature caused the dielectric constant of water to decrease, which in turn resulted in reduced hydration of the solute and the eventual collapse of the humic polymer into a dense aggregate. The final area of investigation was the sorption of perfluorinated surfactants (PFSs) onto a crude humic solid, as well as a high carbon soil. PFSs have gained worldwide attention for their ubiquitous nature and bioaccumulation effects. It was found that their adsorption onto humates is highly dependent pH due to the coulombic nature of the interactions. Both kinetic effects and isothermal sorption characteristics were investigated, and a number of commonly used

models were tested. For the kinetic behavior, neither the pseudo-second order model, nor the intra-particle diffusion model gave entirely satisfactory results. The adsorption isotherms generally followed the Langmuir equation.

Acknowledgements

I would like to thank my mother, Darcy Shaffer, and father, Ralph Shaffer, my aunt and uncle, James and Raenelle Fisher, my grandmother, Margaret Harmening, my brothers and sisters, my friends, and my puppies for all of their support and encouragement.

I would also like to thank my major professor, Ray von Wandruszka for all of his patience, guidance, help and understanding. I would also like to thank Alex Blumenfeld for his assistance and input. Finally, I would like to acknowledge Malcolm Renfrew, and the Renfrew Scholarship for funding assistance, and the University of Idaho faculty and staff.

Dedication

This is dedicated to James Fisher and Darcy Shaffer for always believing in me.

Table of Contents

List of Figures

List of Tables

Chapter One

An Introduction to Humic Materials and the Properties that Allow for Aggregative Behavior and Surface Sorption

1.1 Definition of Humic Materials

Humic materials are the decay products of the total biota in the environment. They consist of a complex mixture of recalcitrant organic substances that defy chemical definition and have been described in a variety of ways. A chemical representation of a typical humic acid can be seen in Fig. 1.1 [1]. Stevenson [2] considered them to be a series of relatively high-molecular weight, yellow to black colored substances formed by secondary synthesis reactions, while Aiken *et al*. [3], described them as a category of naturally occurring, biogenic, heterogeneous organic substances that can generally be characterized as being yellow to black in color, of high molecular weight, and refractory Neither

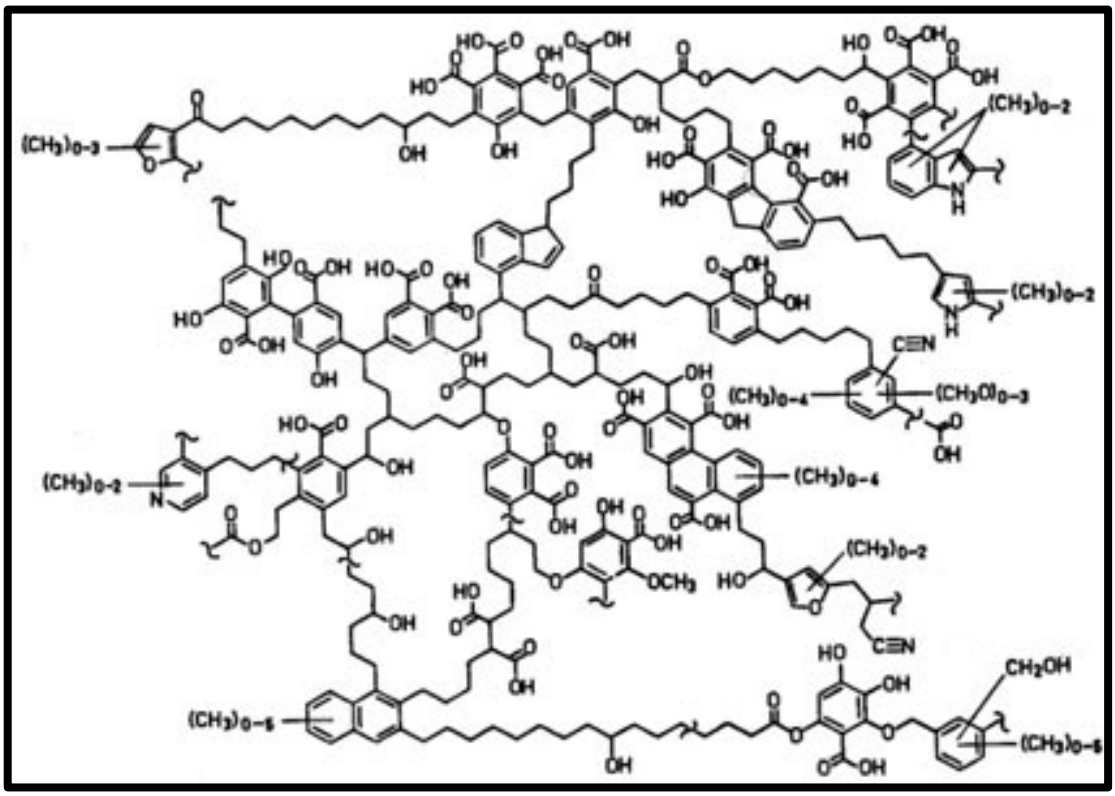

Figure 1.1. Chemical representation of a typical humic acid according to Schulten and Schnitzer [from Ref. 1]

definition is a completely accurate description of humic materials, but they both have been useful for classification and continue to be used by workers in the field.

For practical purposes, humic materials are divided into three operationally defined categories:

1. Humic acid (HA). This is the fraction that is water-soluble at pH values above 2 and consists of a variety of polyanions in the molecular weight range 2,000–20,000 Da. It is generally the major portion of humic materials.
2. Fulvic acid (FA). This is the fraction that is water-soluble at all pH values and consists of smaller, more substituted polyanions in the molecular weight range of500 – 2,000 Da.
3. Humin. This portion is insoluble in water at any pH and while it can be a considerable fraction of the total humic material, it is rarely considered in environmental studies.

In the literature, humic material may be abbreviated 'HM', or referred to as 'humic substances' (HS), or 'soil organic matter' (SOM, a slightly broader category), 'natural organic matter' (NOM, also slightly broader) or simply 'humus'. As humic acid (HA) is the major component of HM, HA (or 'humate') is sometimes used as a *de facto* stand-in for HM. Fulvic acid is abbreviated 'FA'.

1.2 Decomposition Processes and the resulting development of Humic Materials

Humus is the organic component of soils and it can vary greatly in its substitutive and structural properties with location and origin. Humic materials originate in the rhi-

zosphere and their properties are influenced by the environmental factors therein. Factors such as time, climate, amount of vegetation and cropping can exert major influences to the structural properties of humates. Humic material does not accumulate indefinitely in well-drained soils as eventually equilibrium is reached between formative and destructive processes. Climate is the prime determinant in the development of organic matter in soils, due to its influence on microbial activity at a given location. Semi-arid climates lead to the development of grassland soils (mollisols), which are rich in humic materials. Their high organic content is due to a high level of vegetation, an expansive rhizosphere, and harsh conditions that lead to conservation of organic matter.

Organic material tends to decline as soil undergoes cultivation. This is can be attributed to a reduction of plant residues, but also to a stimulation of microbial activity through aeration, leading to accelerated mineralization a volatilization.

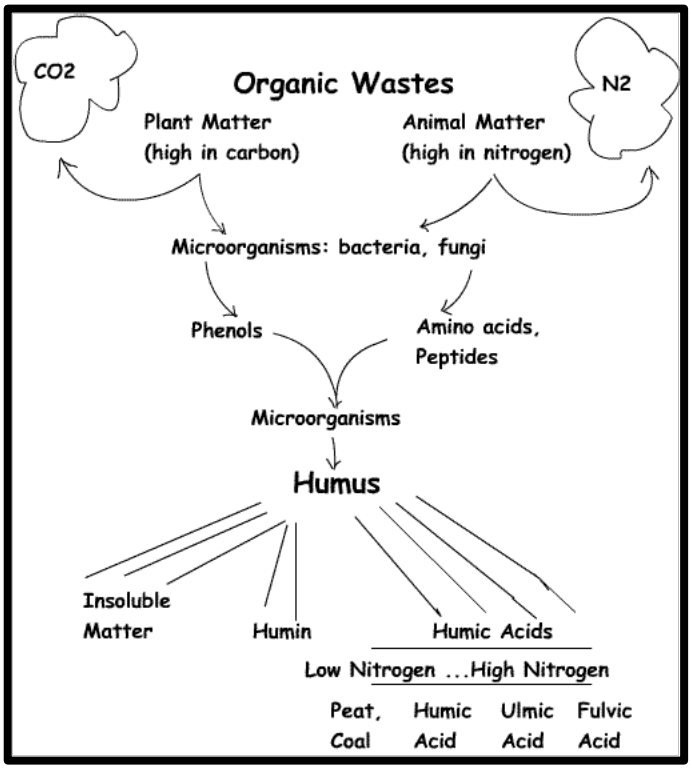

Figure 1.2. Schematic for the conversion of organic waste to humus materials [*illustration accessed at http://oregonbd.org/class-1/*]

As depicted in Fig. 1.2, humic materials are a result of the overall decay process of naturally occurring biota in the environment. Soil animals, such as earthworms, play an important role in the overall reduction of plant material in the environment that leads to further degradation of vegetation carried out via microbial activity in the soil. This stage of the decomposition process is marked by a rapid loss of freely decomposable organic materials. Fungi and actinomycetes then decompose more recalcitrant materials such as lignin and lipids. In cropped soils in temperate zones approximately one third of the carbon material remains behind in the soil after the first growing season, but in time the remaining carbon becomes increasingly resistant to further decomposition [4,5]. This is due to soil organics becoming richer in lignin and other substances with high aromatic content that are much more resistant to decomposition than materials such as cellulose and peptides.

1.3 Biochemical Synthesis of Humic Materials in Soil

There are three major accepted theories for the synthesis of humic materials in soil: (i) the lignin theory; (ii) the polyphenol theory; and (iii) the sugar-amine condensation theory [6-12]. The overall pathways for these theories can be seen in Fig. 1.3. The lignin theory, postulated by Waksman [13], was the predominant theory for the synthesis of humic materials for many years. This theory is currently considered obsolete, but is required for a fundamental understanding of the presently recognized theories.

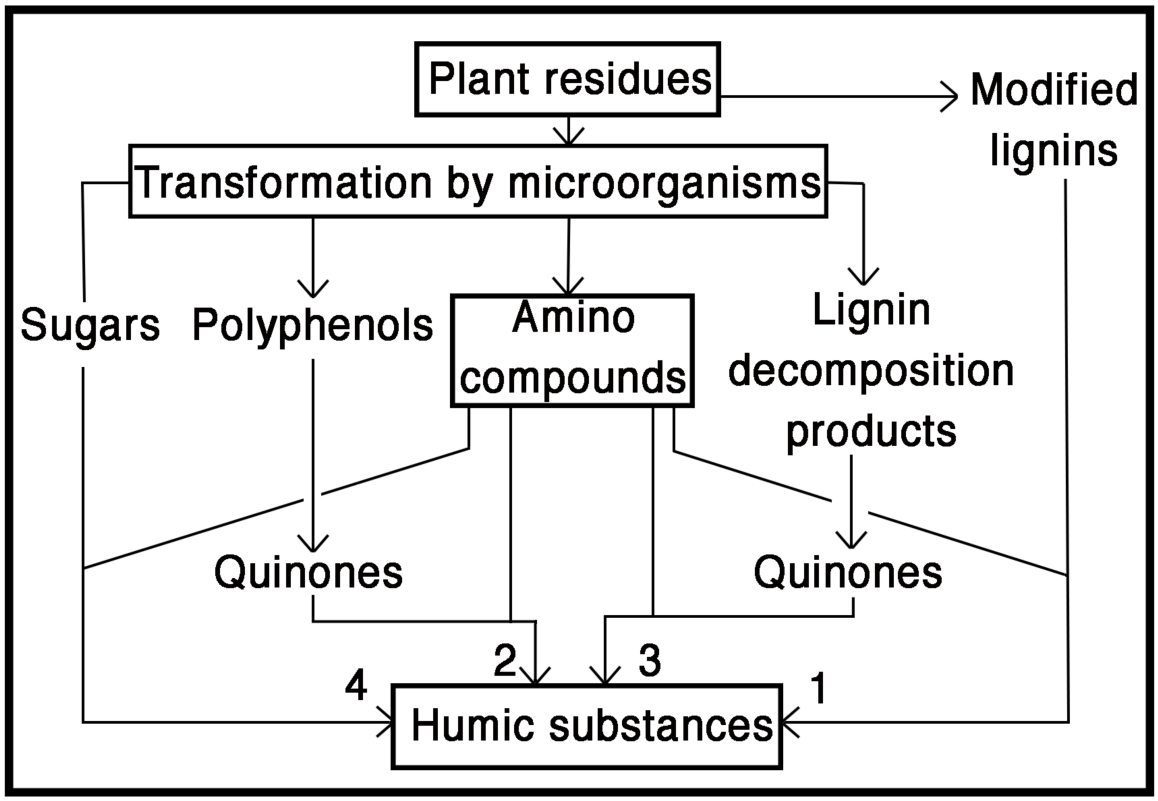

Figure 1.3. Mechanism pathways for the formation of humic materials from plant residue. Pathway 1 is the modified lignin theory. Pathway 2 and 3 are the development of quinones that subsequently transform to humic substances. Pathway 4 is the conversion of sugars to dark colored polymers [from Ref. 13]

1.3.1 The Lignin Theory

The foundation for lignin theory was predicated from some fundamental similarities between lignin and humic materials. The schematic for the overall pathways for the lignin theory is shown in Fig. 1.4. Humic materials and lignin are both decomposed by fungi and bacteria. They are both soluble in alkali solutions and lose solubility in acidic environments. Humic materials and lignin are both acidic in nature, and lignins convert to methoxylated humics when warmed in basic solutions [12,14-16].

As shown in Fig. 1.5, lignins contain phenyl propane units such as coniferyl alcohol, p-hydroxycinnamyl alcohol, and sinapyl alcohol [14-16]. The synthesis of lignin can be broken down to the synthesis of phenylpropane units and the formation of mesomeric free radicals, which lead to the development of lignin intermediates that are then used in the synthesis of humic materials. In this synthetic scheme, glucose that is produced during photosynthesis is converted to p-hydroxyphenyl- and phenyl pyruvic acids that constitute the starting materials for humic substances. From this, larger organic components are formed through a pairing mechanism in which the mesomeric components are created through enzymatic dehydrogenation of the free phenolic alcohol, which leads to the creation of unpaired electrons. These mesomeric free radicals are then paired in a variety of combinations to result in dilignols.

According to this theory, lignin is then converted to humic substances through the loss of methoxy groups, the exposure of the phenolic hydroxyl groups, and the oxidation of terminal side chains in order to create carboxylic groups.

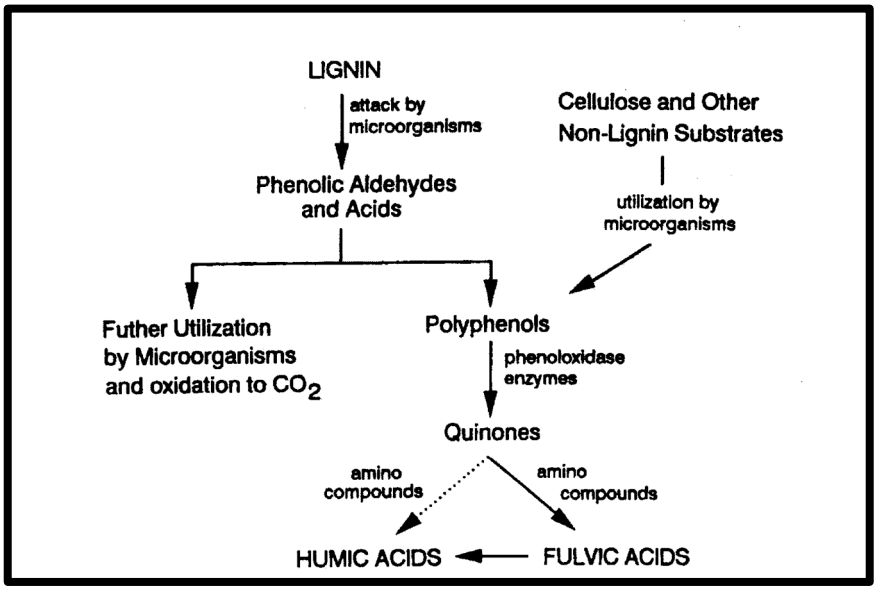

Figure 1.4. Synthetic pathways for lignin building blocks [from Ref. 14]

This process is facilitated by bacteria and microbes, which have the ability to demethylate and oxidize lignin without degrading the polymer. Additional carboxylic groups may arise from the cleavage of the aromatic moieties found in lignin.

A modified lignin theory was postulated by Hatcher and Spiker [9] in which the resistant plant material, *e.g.* lignin, cutin and suberin, and microbial biopolymers evolve into humic materials. This theory is an extension of the one previously discussed, but it includes refractory macromolecules other than lignin.

1.3.2 The Polyphenol Theory

A third theory, postulated by Flaig [17,18], is identified as the polyphenol theory. As Fig. 1.6 shows, quinones derived from lignin and other sources are considered to be the building blocks for the humic substances. The first steps of this synthesic model include the breakdown of plant biopolymers into their monomeric subunits. These monomers then enzymatically, or spontaneously, polymerize to yield humic materials of considerable size and complexity. The smallest units are the fulvic acid, which then develop into humic acid and then possibly into small components of the insoluble humin. The conversion of quinones to humic substances has been observed in the formation of melanin [5,19-22].

Lignin, phenolic plant constituents, glycosides, and tannins serve as the possible sources of phenols. The lignin, which is unlinked from cellulose during the decomposition of plant residue, is split in an oxidative process, which results in derivatives of phenylpropane, which are the primary structural components of the humic material. The

side chains of these building blocks are then oxidized, leading to demethylation and the formation of polyphenols that are in turn converted to quinones. These react with nitrogen containing compounds to form dark colored biopolymers.

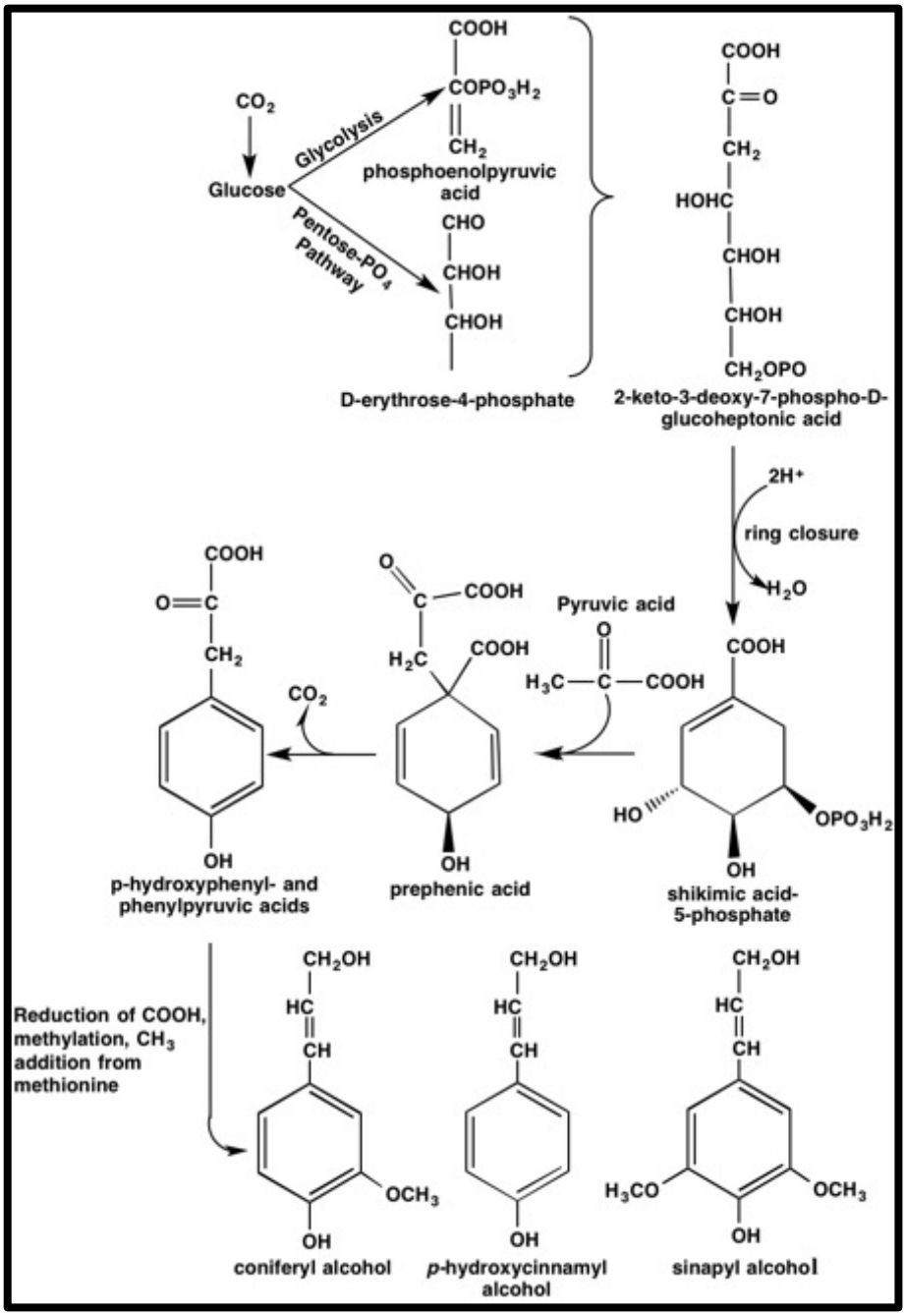

Figure 1.5. Schematic representation of humus formation according to the polyphenol theory [form Ref. 17]

Microorganisms play a role in the formation of the polyphenols. The process of the release of phenols was postulated by Kononova [6] who stated that humic materials were formed in three major stages. The first stage consists of the fungal attack on simple carbohydrates, proteins, and cellulose from plants. In the second stage of this process, the cellulose is decomposed by aerobic mycobacteria. These bacteria then synthesize polyphenols that are oxidized to quinone moieties via polyphenoloxidase enzymes. These quinones subsequently react with nitrogen compounds to form the brown humic materials. In the third stage, the lignin is decomposed, releasing phenols, which continue on as starting materials for humic synthesis.

A schematic showing polyphenols that are also produced during biodegradation of lignin by fungi can be seen in Fig. 1.7. Fungi degrade the lignin in a process that appears as the reverse of its formation. This is due to the initial release of dilignol components and the formation of primary phenylpropane units. These changes occur on the exposed edges of the lignin molecules, catalyzed by extracellular enzymes that are produced by the fungi. This yields common degradation products such as a variety of low molecular weight aromatic acids and aldehydes. Numerous phenol and hydroxyl groups are produced, and different groups are oxidized as well as decarboxylated.

In some environments it is observed that lignin makes no contribution to the polyphenol supply that is used to synthesize humic materials. Under these circumstances, it is believed that the microorganisms themselves contribute the polyphenols to the synthetic process. Many phenolic and aromatic acids can be synthesized from non-aromatic carbon sources. Many species of microorganism such as streptomycetes and

fungi, which are known to populate soils, have been observed to synthesize humic-like substances in solution.

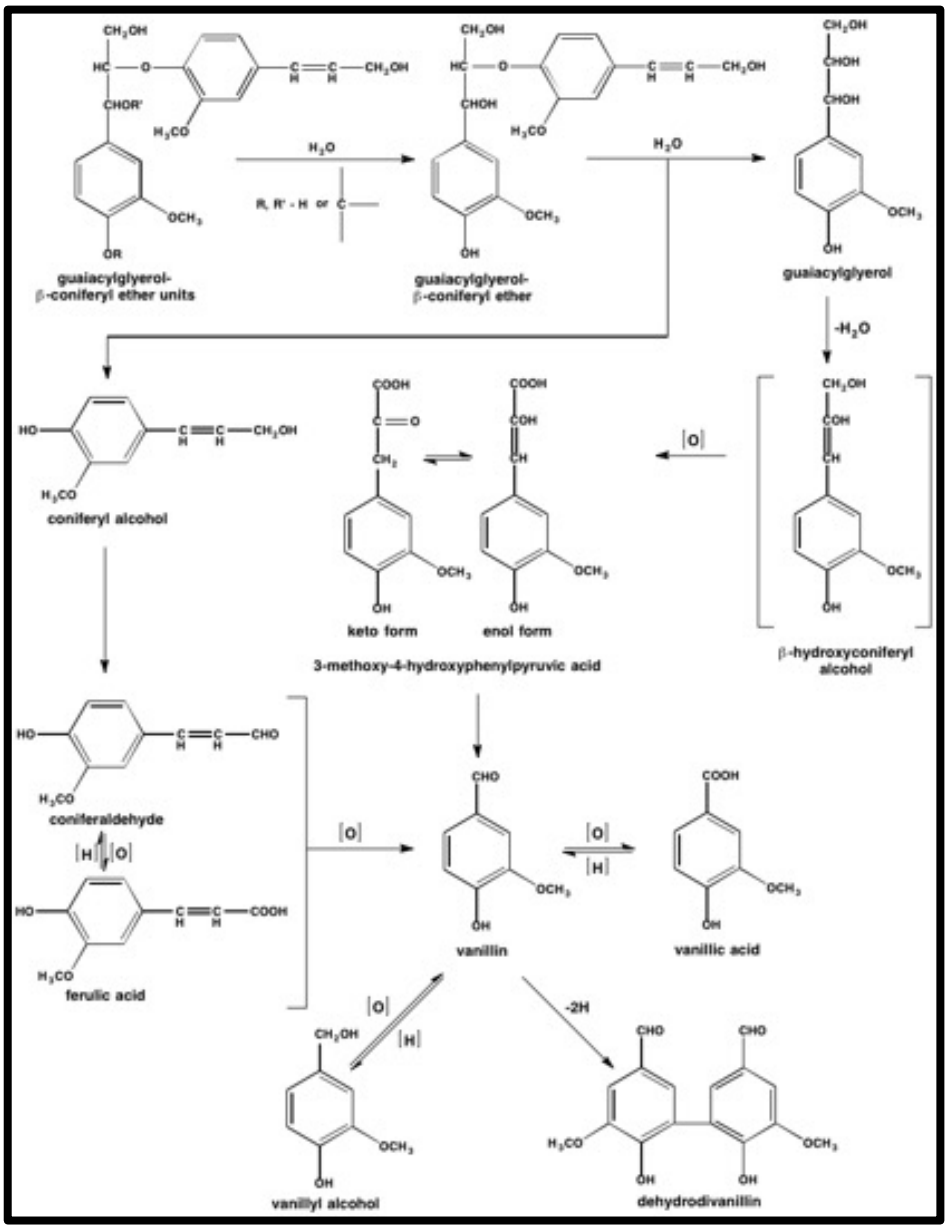

Figure 1.6. Routes of lignin decomposition by fungi according to Schurbert [from Ref 16]

Organic matter has been observed to accumulate in soils saturated with natural gas. This can occur in areas near natural gas wells and in the soil above gas leaks. The carbon materials formed in these events have many of the characteristics of dark-brown humic substances. Their properties include resistance to microbial decomposition, an equivalent total acidity, the same elemental composition, similar total molecular weight, and a tendency to release the same compounds when undergoing degradation.

Microorganisms can degrade cellulose and other organic compounds into macromolecules such as melanin, which arise from phenols synthesized by fungi. The humic materials formed in the absence of lignin do display some differences compared the humic substances that are formed in environments rich in lignins. Humic substances made in their absence contain groups like orsellinic and 2-methyl-3,5-dihydroxybenzoic acids, as well as other phenols, such as resorcinol, that form subsequently.

Once this synthetic process has occurred, the polyphenols can convert into quinone moieties enzymatically. The formation of quinones in humic materials can occur via a variety of pathways, shown in Fig. 1.8. The polyphenols can undergo further decomposition by bacteria, actinomycetes and fungi. In alkaline environments phenolic entities can spontaneously oxidize to quinones, but this is a process more likely to be carried out by polyphenoloxidase enzymes. The result is a vast number of humic products.

The reactions of quinones can be substantially enhanced and varied with the addition of nitrogen containing compounds. When the enzymatic oxidation of phenols

proceeds in nitrogen rich environments, these latter compounds become incorporated into the polymer.

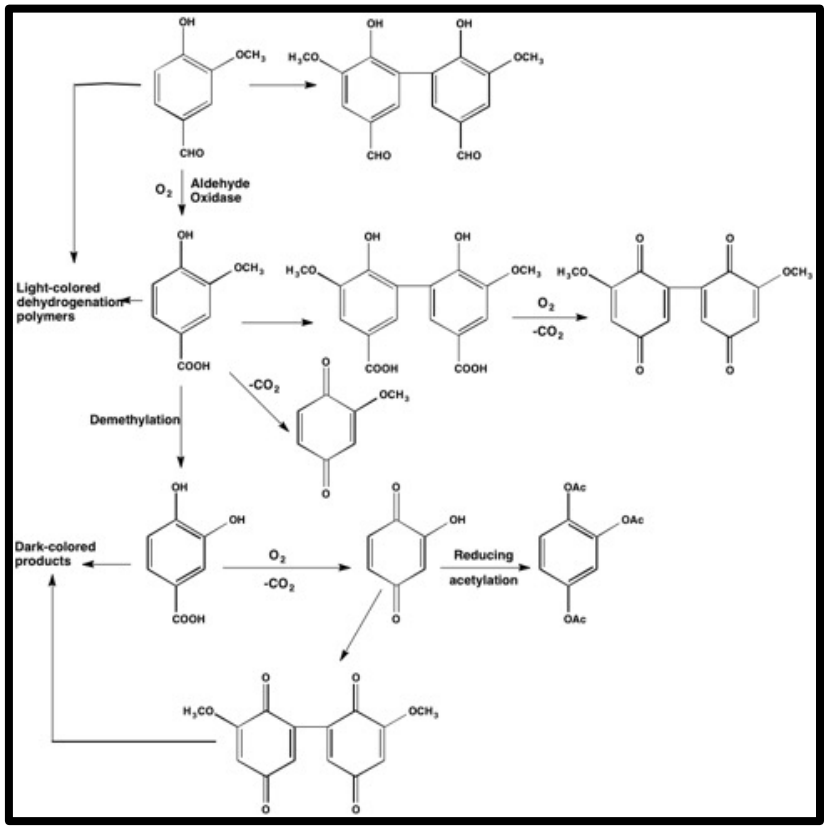

Figure 1.7. Formation of quinones from lignin degradation products according to Flaig [from Ref. 17]

1.3.3 Sugar Amine Condensation

The reactants in the Sugar-Amine Condensation theory are made readily available by microorganisms. The starting reactants, including sugars and amines, are reduced in the dehydration of food products at moderate temperatures. This reaction initially involves the conversion of the aldehyde group on the of the sugar to a Schiff base and an n-substituted glucosamine. As shown in Fig. 1.9 [23] the glucosamine is then converted, via the Amadori rearrangement to an N-substituted-1 amino-deoxyketose. This

product then undergoes fragmentation at which point the ketose loses the amine and then forms chains of aldehydes and ketones. It then loses water to first form reductones and subsequently hydroxymethyl furfural. These products are highly reactive and therefore result in an extremely varied assortment of brown colored products. Aromatic and furanoid moieties are also formed from the carbohydrates. It has been proposed that the conversion of these products to humic substances proceeds via reactions of amino acids and methyl glyoxal. This investigation, by Enders [24], showed that the decomposition process that is carried out by converting amino acids and methyl glyoxal into humic acids.

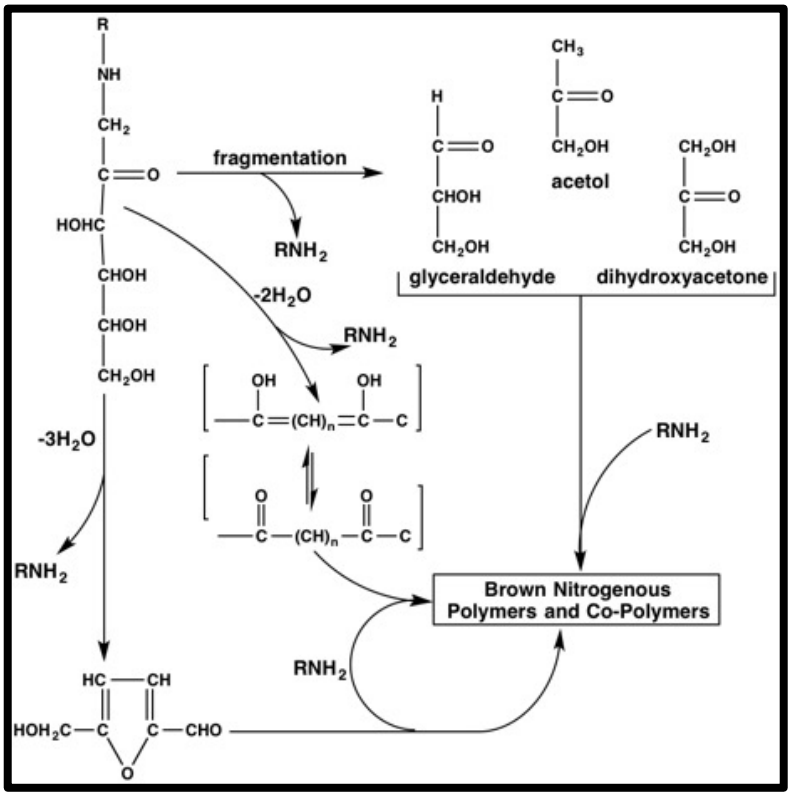

Figure 1.8. Pathways for the formation of brown polymers from the products of the Amadori rearrangement [from Ref. 23]

1.3.4. Summary of Biochemical Synthesis of Humic Materials

Although the Polyphenol Theory is the most widely accepted theory of humate formation [1], it is generally held that all the mechanisms summarized above play a role in the genesis of these materials. In view of the varied nature of the synthetic pathways it is improbable that exactly the same compounds are formed in different situations. It is indeed observed that while all humates display a set of common features and behaviors, there are a seemingly infinite variety of these materials in existence.

1.4 Function of Humic Material in Soil and Its Environmental Benefits

Humic materials greatly affect the physical and structural properties of soils. Humic biopolymer not only function as effective buffers, they also increase water retention, cement clay-sized particles into larger aggregates, promote cation exchange, and even partake in redox reactions.

The presence of humus plays an important role in plant growth. It acts as a carrier in nutritional transport and promotes good soil structure, thereby improving tilth, aeration, and the retention of moisture. Stable humic materials are responsible for the dark color that is observed in many soils and is an important factor in their warming by the sun. Humus helps to minimize soil erosion and acts as a source of energy for soil organisms.

The ability of humic materials to complex other soil components determines many of their environmental effects, from the transport of minerals to the segregation of xenobiotics. They are capable of sequestering heavy metals and thereby reducing

their toxicity to aquatic organisms. Humic materials are involved in ion exchange processes, shown in Fig. 1.10, that are highly specific with regard to the valence of the chelated metals. Monovalent ions can be exchanged with other monovalent ions and divalent metal ions can be exchanged with divalent ions, but a divalent ion cannot be exchanged for two monovalent ions. As a consequence of the exchange mechanism, cations that are plant nutrients are “kept in storage” by being prevented from rapidly leaching out of the soil. As humates bear an overall negative charge, primarily due to their multiple carboxylic groups, they are not effective in the retention of anionic species.

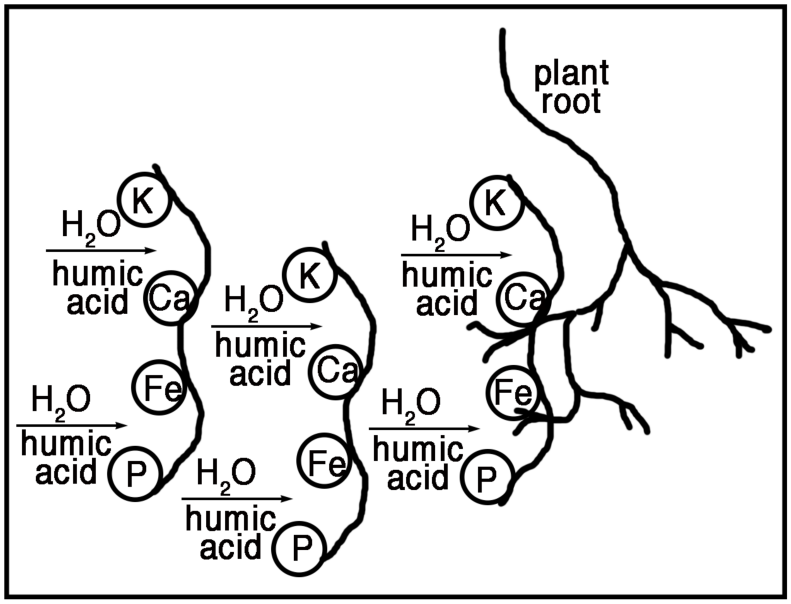

Figure 1.9. Cation exchange process of metal ions that are transported to plant root [*illustration accessed at http://choice-chem.en.alibaba.com/product/744395311-214354025/Humic_Acid_80_.html*]

1.5 Humic Structure and Behavioral Properties

Humic substances are composed of many functional groups that can be categorized as being reactive and non-reactive. The elemental content of humic acids is predominately carbon and oxygen. The carbon content ranges from 53.8 to 58.7 percent and the oxygen content ranges between 32.8 and 38.3 percent. Lesser components include hydrogen, nitrogen and sulfur and they range approximately from 3.2 to 7.0, 0.8 to 4.3, and 0.1 to 3.6 percent respectively.

The major reactive functional groups that contribute to the overall acidity of the humic substance include carboxylic groups, phenolic, enolic, and alcoholic hydroxyl functionalities. Other reactive groups include quinones, ether linkages, free amino groups, and α,β- unsaturated ketones.

The nonreactive, or less reactive, structural components of humic materials include aromatic and lipid regions. Carbohydrate and peptide formations are also found and are usually counted as being of intermediate reactivity.

1.6 Fluorescent Properties of Humic Materials

Humates are fluorescent materials. Their aromatic backbone contains numerous fluorophores, often in conjugated systems, leading to overlapping fluorescent excitation and emission spectra that tend to be broad and featureless [25]. This has placed limits on fluorescence spectroscopy as an analytical tool in the study of humic materials. Typically, excitation at e.g. 240 nm will produce a broad emission band that extends from 300 nm to past 500 nm. In some instances, however, particular fluorescence features

can be singled out and their changes related to molecular processes within the humic structure.

1.7 Surfactant Properties of Humic Substances

Humic materials, especially humic acids, are amphiphilic in nature, and this has given rise to the micellar (or detergent) model for these compounds [26,27]. Various studies [28-35] have indicated that the spontaneous aggregation of aqueous humates can involve a single polymer chain (intra-molecular) or multiple chains (intermolecular). In the intra-molecular case the humic polymers are thought to fold and coil in a manner that creates structured regions that can be likened to knots in a string. The interior of these assemblies is relatively hydrophobic, while the exterior is more hydrophilic. In this manner, the structure is similar to that of a surfactant micelle. It is, however, constrained by the intra-molecular nature of the arrangement and the polydispersity of the material and therefore probably has less uniformity. The term *pseudo-micelle* is more appropriate to describe these structures. A phenomenon similar to the pseudomicelle formation may also be achieved through intermolecular interactions, by the association of a number of humic polymers. The formation of both the intra- and intermolecular species depends on a range of solution conditions, including the concentration and nature of the HA, the pH, the temperature, and the nature and concentration of cationic species present in solution. It has been shown that metal ions, especially polyvalent ones, have a major influence on humic aggregation and the formation of pseudomicellar structures.

1.8 Sorption Processes of Humic Materials

Solid humic materials in contact with aqueous solutions frequently are able to adsorb solutes from these solutions. A number of bonding interactions may occur between adsorbent and adsorbate, including physical bonding, electrostatic bonding, H-bonding, and coordination [1].

Physical bonding involves van der Waals forces and result in a weak interaction between species, due to electrical charge fluctuation. A positive fluctuation in one partner induces a negatively fluctuation in another, resulting in a weak attraction between them. This is a major contributor to the adsorption of neutral and nonpolar compounds to similar regions in the humic structure.

Another type of bonding that can be important in the adsorption processes various species onto humic materials is electrostatic bonding. This occurs either via a cation exchange process, or the protonation of carboxylic groups on the humic substance. The status of the interaction site on both adsorbent and adsorbate is often pH sensitive, and this parameter therefore tends to have an influence on the adsorption [36].

Hydrogen bonding and coordination are other mechanisms by which adsorption can occur. Hydrogen bonding occurs through the linkage of two electronegative atoms. Hydrogen has a high tendency to share electrons with atoms that contain unpaired electrons. This interaction can assist in the adsorption between protonated molecules and surface hydroxyls. Metals ions can bind to nonmetal organic sites through coordination or charge transfer complexes. In doing so, the metal ion forms a bridge between the adsorbate molecule and the humate.

1.9 References

[1] Schulten HR, Schnitzer M. A State of the Art Structural Concept for Humic Substances. Naturwissenschaften 1993; 80:9–30.

[2] Stevenson FJ. Humus chemistry: genesis, compositions, reactions. 2nd ed. John Wiley and Sons, Inc., New York, NY, 1994.

[3] Aiken GR, McKnight DM, Wershaw RL, MacCarthy P. in Humic Substances in Soil, Sediment, and Water: Geochemistry, Isolation, Characterization. Aiken, G.R. et al. (eds.). John Wiley and Sons, Inc., New York, NY, 1985.

[4] Jenkinson DS. Studies on the Decomposition of Plant Material in Soil II. Partial Sterilization of Soil and the Soil Biomass. J. Soil Sci. 1966; 17:247.

[5] Jenkinson DS. Studies on the Decomposition of Plant Material in Soil I. Losses of Carbon FROM ^{14}C Labeled Ryegrass Incubates with Soil in the Field. J. Soil. Sci. 1965; 16(1):104.

[6] Haider K, Martin JP, Filip Z. Humus Biochemistry. Paul EA, and McLaren AD, Eds. Soil Biochemistry. Vol. 4. Mercer Dekker, New York 1975, 195-244.

[7] Kononova MM. Soil Organic Matter. Pergamon, Oxford 1966.

[8] Martin JP, Haider K. Microbial Activity in Relation to Soil Humus Formation. Soil Sci. 1971; 111:54-63.

[9] Flaig W. Generation of Model Chemical Precursors. Frimmel FH, Christman RF, Eds., in Humic Substances and Their Role in the Environment. Wiley, New York 1988, 75-92.

[10] Hatcher PG, Spiker EC. Selective Degredation of Plant Biomolecules. Frimmel FH, Christman RF, Eds., in Humic Substances and their Role in the Environment. Wiley, New York 1988, 59-74.

[11] Hedges JI. Polymerization of Humic Substances in Natural Environments. F.H. Frimmel and R.F. Christman. Eds., in Humic Substances and their Role in the Environment. Wiley, New York 1988, 45-58.

[12] Francois R. Marine Sedimentary Humic Substances: Structure, Genesis, and Properties. Reviews in Aquatic Sciences. 1990; 3:41-80.

[13] Waksman SA. Humus. Williams and Wilkins, Baltimore, 1932.

[14] Crawford HA. Lignin Biodegradation and Transformation. Wiley, New York, 1981.

[15] Pearl IA. Lignin Chemistry. Chemistry & Engineering News. 1964; 42(27):81-92.

[16] Schubert WJ. Lignin Biochemistry. Academic Press, New York, 1965.

[17] Flaig W. The Chemistry of Humic Substances. The Use of Isotopes in Soil Organic Matter Studies. Report of FAO/IAEA Technical Meeting. Pergamon, New York. 1966, 103-127.

[18] Flaig W, Beutelspacher H, Rietz E. Chemical Composition and Physical Properties of Humic Acids. Gieseking JE. Ed., Soil Components: Vol 1. Organic Components. Springer-Verlag. New York 1975, 1-211.

[19] Haider K, Martin JP. Synthesis and Transformation of Phenolic Compounds by Epicoccum nigrum in Relation to Soil Humus Formation. Soil Sci. Assoc. Amer. Proc. 1967; 31:766-772.

[20] Haider K, Martin JP. Humic Acid-Type Phenolic Polymers from Aspergillus sydowi Culture Medium, Stachybotrys spp. Cells and Autoxidized Phenol Mixtures. Soil Biol. Biochem. 1970; 2:145-156.

[21] Martin JP, Haider K, Wolf D. Synthesis of Phenols and Phenolic Polymers by Hendersonula toruloidea in Relation to Soil Humus Formation. Soil Sci. Soc. Amer. Proc. 1972; 36:311-315.

[22] Saiz-Jimenez C, Haider K, Martin JP. Anthraquinones and Phenols as Intermediates in the Formation of Dark-Colored Humic-Like Pigments 1975. Soil Sci. Soc. Amer. Proc. 1975; 39:649-653.

[23] Maximov OB, Glebko LI. Quinoid Groups in Humic Acids. Geoderma, 1974; 11:17.

[24] Ender C, Sigurdsson S. Uber den Chemismus der Huminsaurebildung Unter Physiologischen Bedingungen. VII Mitteilungen. Biochem. Z. 1947; 318:44-46.

[25] Schnitzer M, Khan SU. Humic Substances in the Environment. Marcel Dekker, Inc., New York 1972.

[26] Wershaw RL. A New Model for Humic Materials and Their Interactions with Hydrophobic Organic Chemicals in Soil-Water or Sediment-Water Systems. J. Contam. Hydrol. 1986; 1: 29-45.

[27] Wershaw, RL. Model for humus in soils and sediments. Environ. Sci. Technol. 1993; 27(5): 814-816.

[28] Puchalski MM, Morra MJ, von Wandruszka, R. Fluorescence Quenching of Synthetic Organic Compounds by Humic Materials. Environ. Sci. Technol. 1992; 26:1787-1792.

[29] Engebretson RR, von Wandruszka R. Micro-organization in Dissolved Humic Acids. Environ. Sci. Technol. 1994; 28(11):1934-1941.

[30] Engebretson RR , von Wandruszka R. Quantitative Approach to Humic Acid Associations. Environ. Sci. Technol. 1996; 30(3):990-997.

[31] Engebretson RR, von Wandruszka R. The Effect of Molecular Size on Humic Acid Association. Org. Geochem., 1997; 27(11-12):759-767.

[32] Ragle C, Engebretson RR, von Wandruszka R. The Sequestration of Hydrophobic Micropollutants by Dissolved Humic Acids. 1997; Soil Sci., 162(2):106-114.

[33] von Wandruszka R, Ragle C, Engebretson RR. The role of Selected Cations in the Formation of Pseudomicelles In Aqueous Humic Acid. 1997; Talanta, 44:805-809.

[34] Yates III L.M, Engebretson RR, Haakenson TJ, von Wandruszka R. Immobilization of Aqueous Pyrene by Dissolved Humic Acid. Anal. Chim. Acta. 1997; 356:295-300.

[35] Yates III LM, Ray von Wandruszka R, Effects of pH and Metals on the Surface Tension of Aqueous Humic Materials, Soil Sci. Soc. Am. J., 1999; 63:1645–1649.

[36] Chiou CT. Theoretical Considerations of the Partition Uptake of Nonionic Organic Compounds by Soil Organic Matter. B.L. Sawhney and K. Brown. Eds, Reactions and Movement of Organic Chemicals in Soils. Special Publication 22. Soil Science Society of America, Madison. 1989, 1-29.

Chapter Two

Experimental Procedures and Preliminary Characterization

2.1 Introduction

Humic materials are a diverse suite of natural polymers with a great variety of functional groups. It is important to consider the moiety of interest when choosing an analytical technique to investigate a particular behavior or characteristic of these materials.

The work presented in the following chapters features a number of analytical techniques, which helped to elucidate the aggregative behavior of humic materials in aqueous solution. The analytical techniques used in this body of work were chosen specifically for the ability to offer information regarding this aggregative effect and the subsequent effects that resulted from them.

The first task at hand in a study of humates is their isolation from the natural matrix – soil in the present case – and their characterization by the appropriate techniques.

2.2 Isolation of Humic Substances

The nature and quantity of humus in soil depends on the environment from which it originates. Latahco Silt Loam Humic Acid (LSLHA) was isolated from a silt loam (Argiaquic Xeric Argialbolls) found in Latah County, Idaho. A mass of 600 g of soil was subjected to a series of chemical processes [1], which are described below, in order to isolate the humic content, a schematic for this procedure can be seen in Fig. 2.1.

First, the soil was subjected to an acid wash, in which it was placed in a 0.1 M HCl solution (10 mL solvent per 1 g of soil) and shaken for 1 h on a Newbrunswick Scientific

Reciprocal Water Bath Shaker. The supernatant was separated from the residue by decantation, followed by centrifugation. The supernatant, which contained a small amount of fulvic acid, was discarded.

The residue was neutralized with a 1.0 M solution of NaOH until the pH reached 7, and then a 0.1 N NaOH solution was added until the solid : solvent ratio was again 1:10. The sample was shaken, this time for 4 h, and the suspended particulates were allowed to settle. The supernatant was decanted and acidified with a solution of 6 M HCl while being constantly stirred until it reached a pH of 1.0. The solution was left to stand for 12-16 h and was centrifuged in order to separate the humic acid from the dissolved fulvic acid fractions.

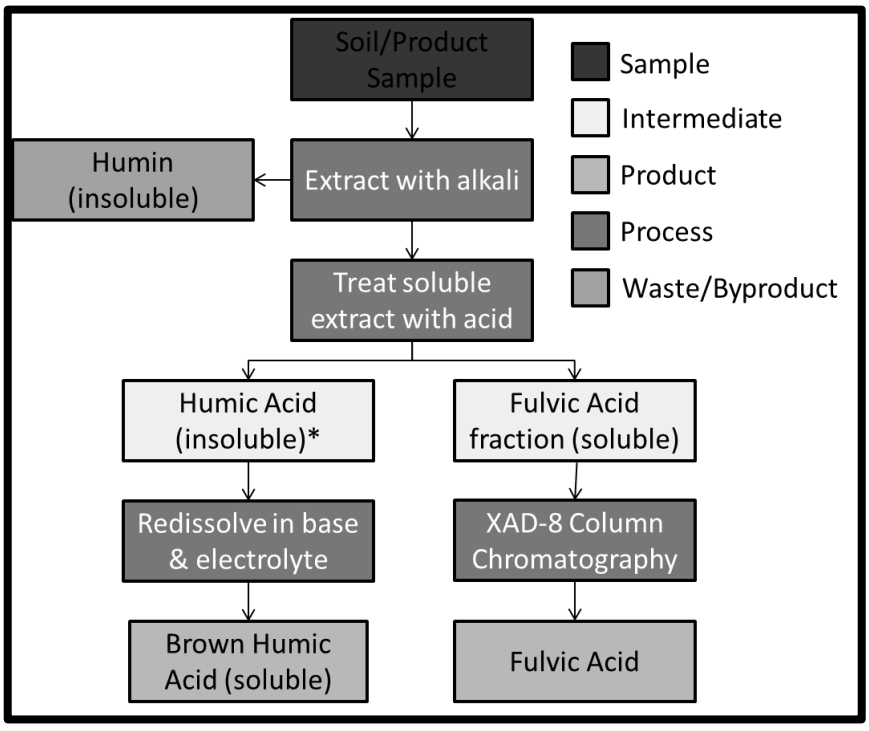

Figure 2.4. Scheme for the isolation of humic substances from soil [Adapted from Stevenson (1994)]; *California Department of Food and Agriculture (CDFA) testing process end point. Accessed: http://dirtmd.com/standard-humic-acid-testing-protocols-a-review/

The humic acid was redissolved by adding a minimum volume of 0.1 N KOH. KCl was added until the potassium concentration was 0.3 M, and suspended solids were removed by centrifugation. The humic fraction was reprecipitated by adding 6 M HCl with constant stirring until a pH 1.0. The suspension was centrifuged and the supernatant discarded. The solid humate was demineralized by placing it in a solution of 0.1 M HCl and 0.3 N HF in a plastic container, shaking it, and leaving it overnight at room temperature. The sample was transferred to dialysis tubes and put into a tank of deionized water, which allowed chloride to pass from the sample pouch to the water tank. A silver nitrate solution was used to test the water for chloride and when the test was negative, the sample was freeze-dried. This isolation procedure yielded 2 g of humic acid from 600 g of soil.

2.3 Acid Content Determination by Conductivity Measurements

When humic polymers in aqueous solution undergo intramolecular "aggregation", as they do when the ionic strength is increased [2], they contract into more tightly folded shapes and thereby become more mobile:

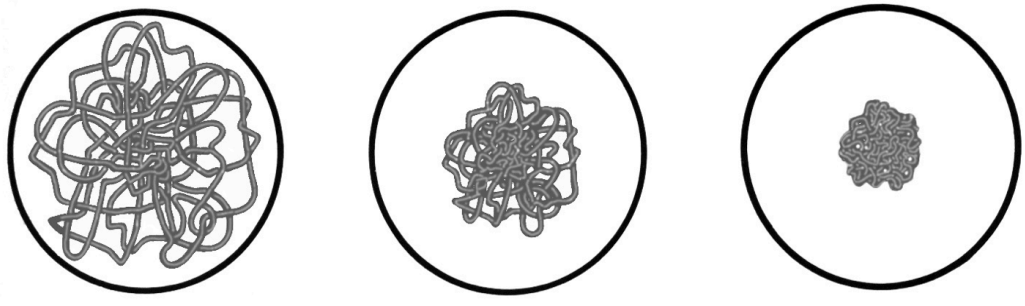

This greater mobility manifests itself in an increase in conductivity. Conductivity measurements can be used to determine the acid content of the humic polymers [2,3]. Humic material goes into solution when an alkaline environment is provided and the carboxylic groups are deprotonated. This causes repulsion between the aliphatic chains and the humate "stretches out" into the fully expanded form shown in the illustration above.

Humic acid solutions were prepared by adding a minimal amount of NaOH to an aqueous suspension of the humate. Once the material was completely dissolved, an excess of approximately 5 µeq of hydroxide was added. This slightly basic humate solution was then titrated with 0.0125 N HCl.

The HCl titrant was added to a titrant chamber of a Titronic Universal Automatic Titrator (Schott), which dispensed it in 50 µL aliquots every 30 s under constant stirring. The titration vessel contained 27 mL of the aqueous humate solution and its conductivity was measured using a Hanna four-ring platinum electrode connected to a Hanna Instruments 2315 Conductivity Meter. A Vernier Labpro data logger captured the signal and relayed it to a computer.

As shown in Fig. 2.2, the initial solution conductivity was relatively high because of the excess hydroxide. As the neutralization proceeded, the OH^- ions were effectively replaced by Cl^- ions, and since the respective equivalent limiting conductance ($\boldsymbol{\Lambda_{eq}}$) values of these two species are 199.2 S cm^2/eq and 76.35 S cm^2/eq the overall conductance of the solution decreased. A conductance minimum was reached when the excess OH^- was consumed. After this point, the HCl titrant progressively protonated the hu-

mate itself, replacing humate with chloride. As Cl^- is smaller and more mobile than the humate, the former has a somewhat larger Λ_{eq} and the solution conductance rose again – albeit slowly. After protonation of the humate, subsequent addition of HCl added both H+ (Λ_{eq} =350.1 S cm^2/eq) and Cl− to the solution, resulting in a sharp rise in conductance. The number of acid equivalents corresponding to the slow-rising portion of the titration curve was taken to represent the acid equivalents in the humic acid [4].

In this manner the conductivity titration curves were used to determine the total acid content of the humic acid under investigation. A number of determinations were carried out in order to characterize Latahco silt loam humic acid (LSLHA), which was the primary material used in all subsequent studies. Size fractions of LSLHA were separated by ultrafiltration with an Amicon Ultrafiltration device. The curves for two of these (500-3000 Da and 50K-100K Da) are displayed in Fig 2.5. The conductance titration curve of photolyzed LSLHA was also generated. Photolysis was carried out by placing a 200mg/L humate solution into a Rayonet Photochemical Reactor chamber for 48 h. This caused the humic polymers to break into smaller fragments [5].

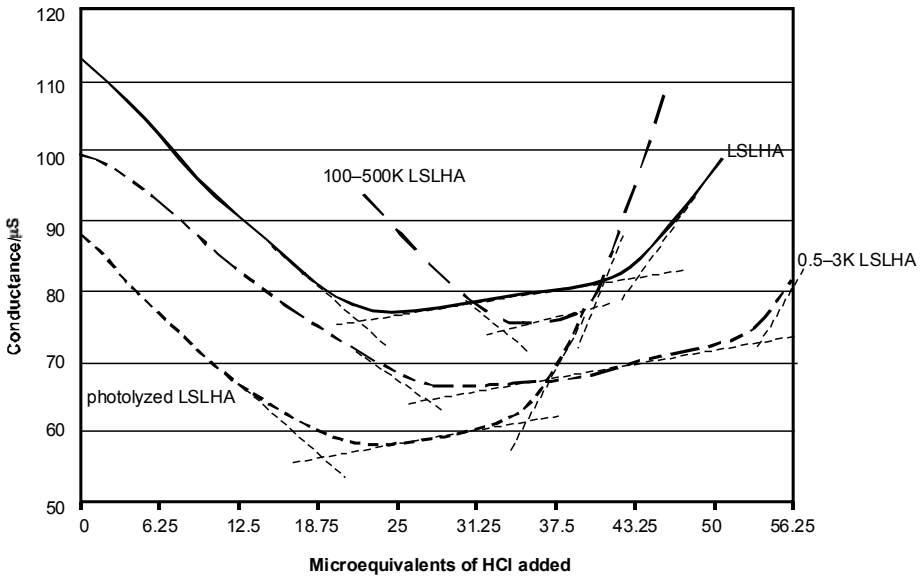

Figure 2.5. Conductometric titration curve for determination of acid equivalencies in LSLHA.

The humate solutions used all had a volume of 27.0 mL and contained the following quantities of solute: LSLHA 3.5 mg; 0.5K–3K fraction 2.8 mg; 50K–100K fraction 0.8 mg; photolyzed material 1.8 mg. The respective acid contents were determined to be:

- untreated LSLHA: 6.52 meq/g
- smaller size fraction: 9.64 meq/g
- larger size fraction: 8.82 meq/g
- photolyzed material: 15.0 meq/g

2.4 Determination of pK_a

The pK_a of LSLHA was determined with a standard titration curve using a pH electrode. This technique did, however, present a fundamental problem: Humic polymers, especially the larger ones, tend to adhere to the glass bulb of the electrode and thereby produce incorrect readings [4]. To avoid this, the probe was placed in a dialysis bag that let the solvent pass freely, but prevented the humic material from reaching the membrane. The titration curve obtained (Fig. 2.3) was similar in shape to those of polyprotic acids, which is consistent for humic materials. The inflection point in the first buffer region corresponded to the pK_a of the stronger acid moieties (approx. 2.6) and the inflection point in the second buffer region (approx. 6.5) indicated the pKa of the weaker acid groups.

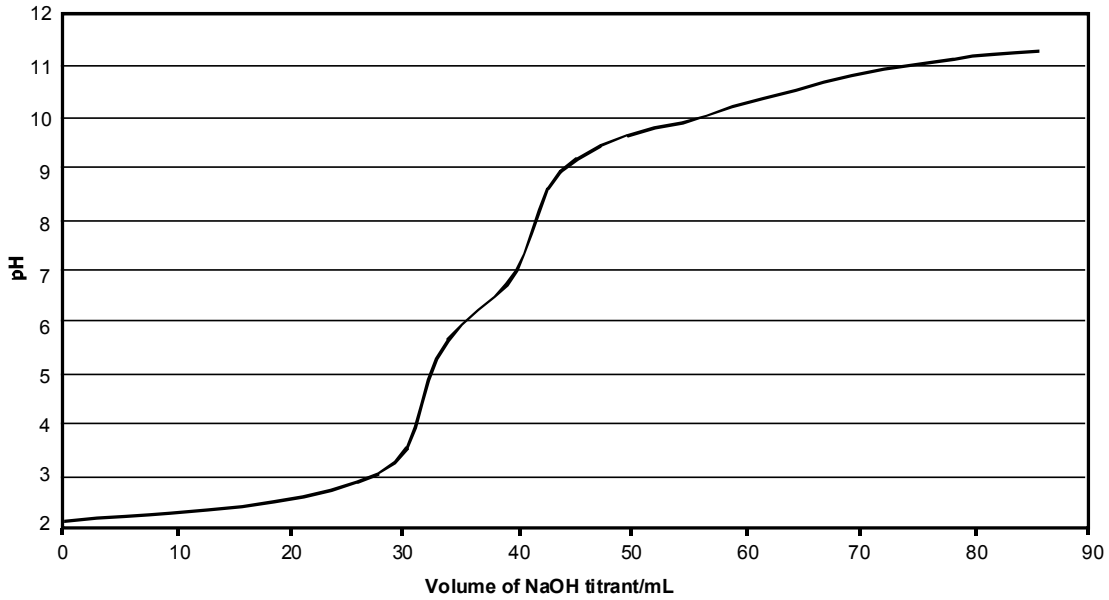

Figure 2.6. Titration curve for LSLHA. Titration carried out using a 40 mg/L solution of LSLHA acidified to a pH just above 2 using 0.04 M NaOH

2.5 Fluorescence Spectroscopy

A variety of different fluorescence techniques have been employed to gain analytical information about humic materials. These include standard excitation fluorescence, synchronous scan fluorescence [6,7], florescence quenching, luminescence sensitization [8], and the use of fluorescent probes such as pyrene [9]. Fluorescence has been a valuable technique in determining the presence of quinones [10], which are among the strongest fluorophores commonly found in the humic structure. Fluorescence has been significant to the research discussed below with particular emphasis on the detection of quinone moieties and pyrene fluorescence probing.

Fluorescence measurements were taken with a Horiba Jobin-Yvon Fluorolog-3 fluorimeter and supplemented by a Hitachi F-4500 fluorescent spectrophotometer and a SLM-Aminco 8100 fluorimeter. Humic materials are rich in fluorophores. Many of these, including the quinones, are structurally similar, which results in an overall spectrum that

is composed of several similar overlapping peaks. As shown in Fig. 2.4, the fluorescent spectra of humic materials therefore tend to be broad and featureless, limiting their analytical use.

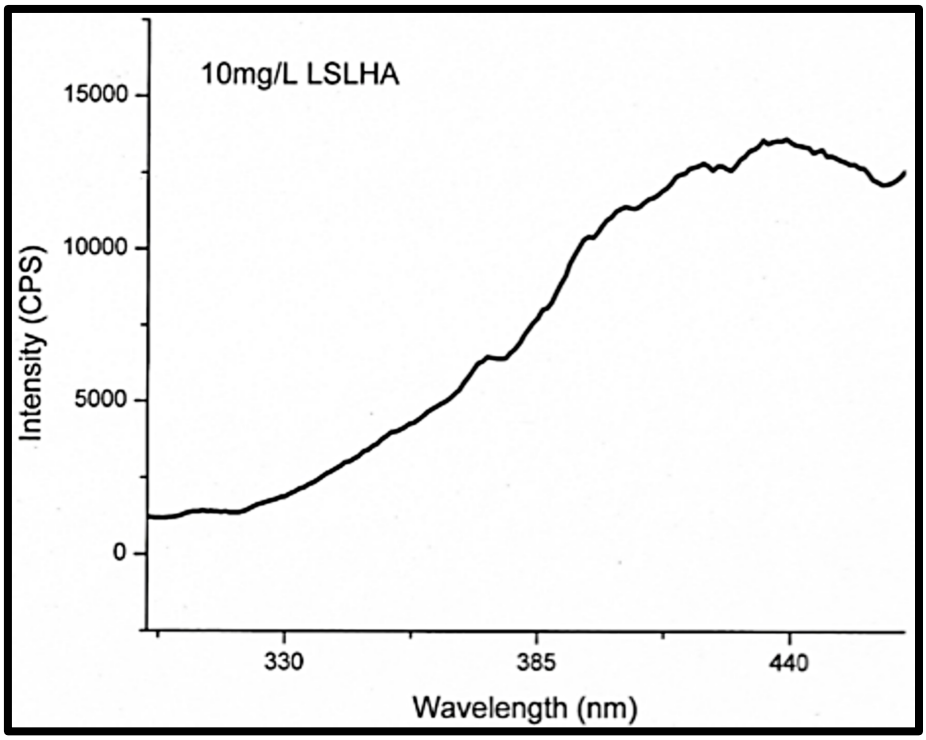

Figure 2.7. Fluorescent spectrum of 10 mg/L LSLHA when excited at 240 nm

Quinones are excited at 240-245 nm range and give an emission peak at 400 nm, shown in Fig. 2.5. The emission is readily quenched by water. The concentrations of the humic solutions created for the studies described here typically ranged from 10 to 60 mg/L. Three milliliter aliquots of these solutions were added to a quartz cuvette and placed in a sample chamber that was thermally regulated at a constant temperature of 25^{o} C. The sample was excited using xenon-arc lamp and an emission spectrum between 300 to 465 nm was obtained at a 90^{o} angle to the excitation beam. The fluorescent

spectra were taken in triplicate and smoothed using a Savitzky-Golay smoothing algorithm.

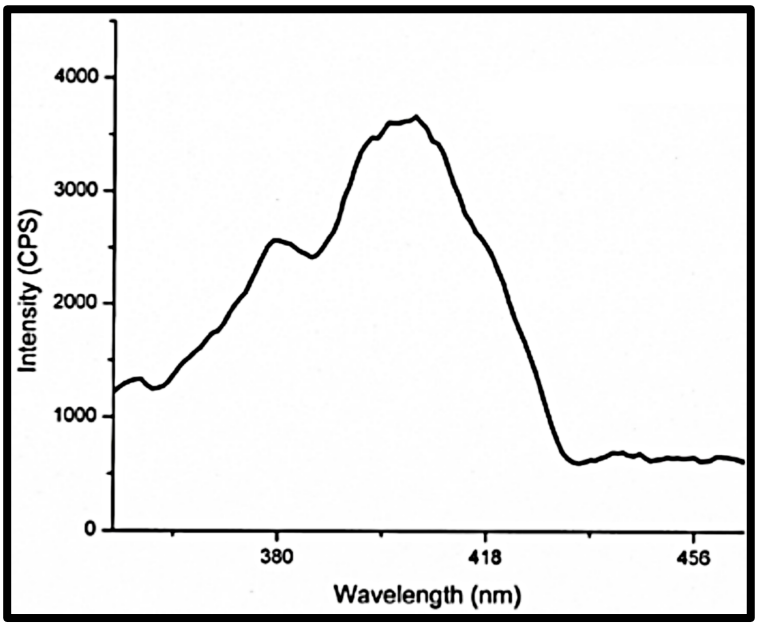

Figure 2.8. Fluorescent spectrum of *p*-quinone when excited at 240nm.

A pyrene fluorescent probe was used to follow aggregation and micellization of humic solutes in aqueous solution. When pyrene is excited at 240 nm it produces a distinct emission spectrum that can be used to determine the polarity of the pyrene environment [11].

The pyrene spectrum has five vibronic peaks, shown in Fig. 2.6. The ratio of the first (I_1) and third (I_3) vibronic peak height can be used to determine the polarity of the pyrene environment. This I_1/I_3 ratio ranges from 0.8 to 1.6, where the value of 0.8 occurs in a nonpolar environment such as hexane, and the value of 1.6 occurs in a polar environment such as water. The I_1 peak is formally spin forbidden, but in a polar environment it is enhanced due to spin-orbit coupling. In a nonpolar environment, however,

the I_1 peak is relatively small. The I_3 peak is not affected by the polarity of the environment. Thus, pyrene can be used as a probe to indicate the polarity of this environment. This phenomenon was exploited to assess the sequestration of pyrene in the humic aggregates.

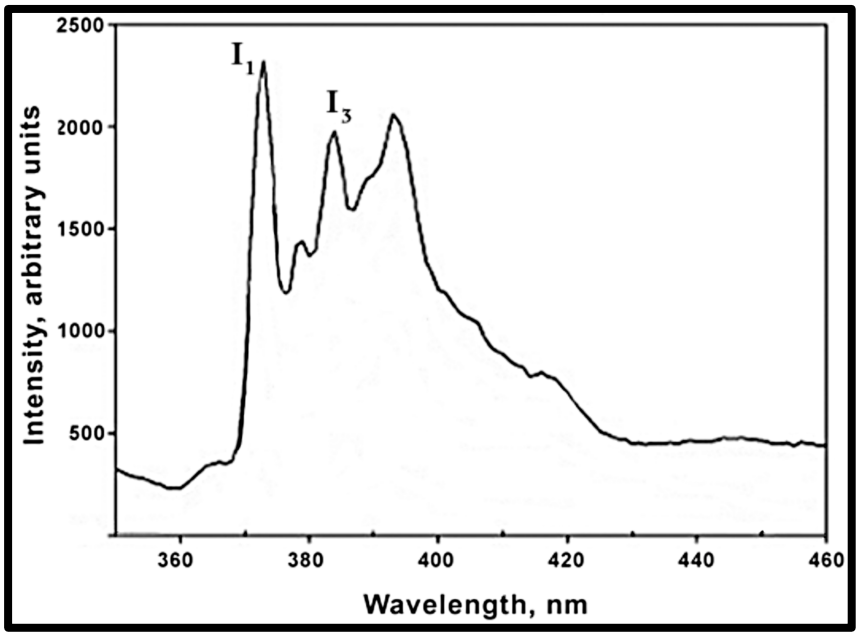

Figure 2.9. Fluorescent spectrum of pyrene when excited at 240 nm. The first and third vibronic peaks labeled I_1, and I_3, respectively

2.6 Particle Sizing

Dynamic light scattering is a technique that can be used to measure the average size and polydispersity of particles in a suspension. The dynamic light scattering instrument detects the fluctuations of interfering light scatted radiation and uses these to determine particle sizes. A beam of light of fixed wavelength (640 nm emission of a He-Ne laser) is used to illuminate particles in random, or Brownian, motion. As they scatter this light, an interference pattern is created that fluctuates depending on how rapidly the

particles move in solution. Fast moving particles cause a more rapidly fluctuating interference pattern than slow moving particles, Fig. 2.7. The instrument uses this information to determine the diffusion coefficient of the particles, and then uses the Stokes-Einstein equation $\left[d = \frac{k_B T}{3\pi\eta D}\right]$[1] to calculate the average particle size [12].

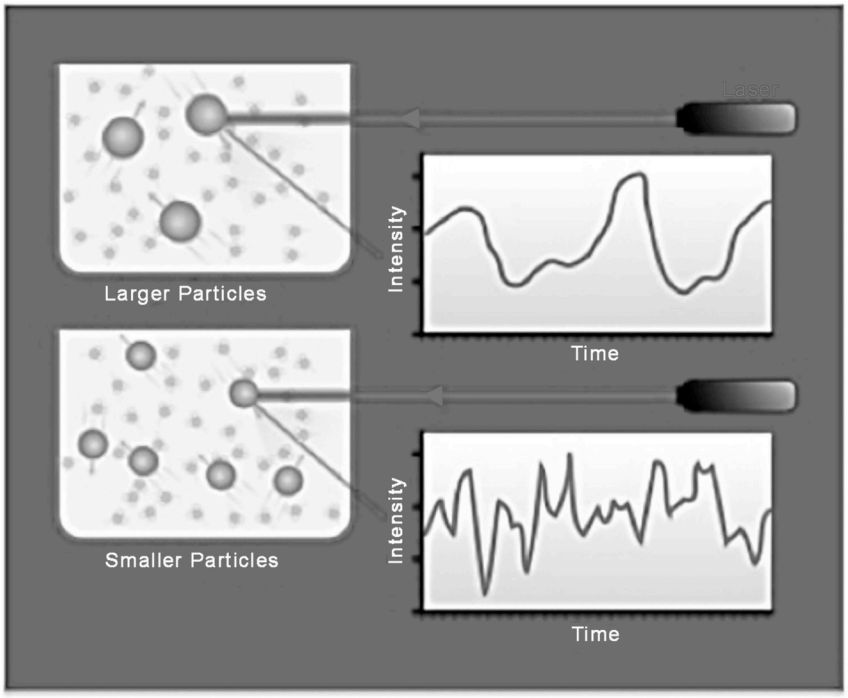

Figure 2.10. Hypothetical illustration of dynamic light scattering of a large particle and a small particle. Image created by Mike Jones at Creative Commons, accessed at http://www.quantachrome.co.uk/en/dynamic-light-scattering.asp#dlsimage

A Coulter N4 Plus Particle Size Analyzer was used in this work to determine the particle sizes of humic aggregates as they changed in response to various solution parameters. The instrument was calibrated with standard suspensions of latex particles of known size.

[1] d=particle diameter ; k_B=Boltzmann const.; T=temperature; η=viscosity; D=diffusion coefft.

2.7 Adsorption

Kinetic and isotherm data was collected for adsorption processes between humic material and perfluorinated surfactants (PFS). The procedure for the kinetic experiments involved using 20 mL portions of a 0.002 M solution of perfluorinated surfactants. The PFS was the adsorbate and the humic material was the adsorbent. An SEM for the surface of a humic acid can be seen in Fig. 2.8. The PFS that were commercially available for investigation were perfluorooctane sulfonic acid (PFOS) and perfluorooctanoic acid (PFOA).

PFS are of particular interest because they have been of growing concern from an environmental standpoint. PFOS and PFOA are man-made chemicals that are extremely persistent in nature. A common source of PFOS is Teflon production and PFOA can be sourced to Scotchguard products [13]. However, the interest of these studies is based on the use of these PFS materials as a key ingredients in flame-retardants used in fighting wildfires.

The adsorbent was an 80% crude blend Leonardite Humic Acid (LHA), which is commercially sold as a soil conditioner. It was used as a typical humate that may be found in the environment and with which PFS may interact. The material was passed through a five-millimeter sieve to remove larger particles.

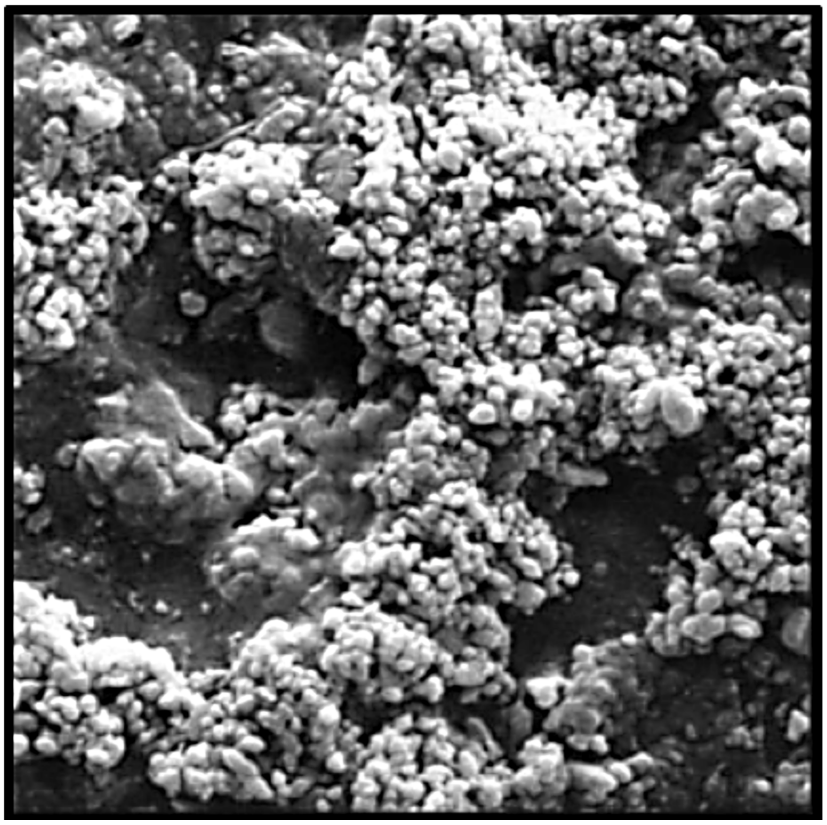

Figure 2.11. SEM image (approx 2000x) of a solid humic acid. Accessed at http://www.northeastern.edu/hagroup/about/

2.7 ^{19}F NMR

Humic materials absorb light at all wavelengths, making it difficult to quantify PFS in humic solutions by spectroscopic means. Humic materials also have surfactant properties, which hinders their chromatographic separation from PFS. However, PFS are fluorine rich whereas humic materials do not contain fluorine. Therefore, ^{19}F NMR was a suitable detection technique for the kinetics and isotherm experiments.

The perfluorinated surfactants of interest were in aqueous solution, and the NMR signal was locked to a standard by the incorporation of a central probe with deuterated DMSO in the NMR tube containing the PFS analyte.

Depending on the level of adsorption in the experiment under consideration, the NMR tube contained at times very low concentrations of PFS. This meant that the NMR spectrum had to be acquired over a period of several hours. All solutions were run for the same period of time and the large triplet peak that represented the terminal CF_3 group of the perfluorinated surfactant was integrated to determine the percentage of the perfluorinated surfactant that remained in solution.

2.8 References

[1] Stevenson FJ. Humus Chemistry: Genesis, Composition, Reactions. J. Wiley, New York, 1994.

[2] Young C, von Wandruszka R. A Comparison of Aggregation Behavior in Aqueous Humic Acids. Geochem. Trans. 2001; 2:16-20.

[3] Andjelkovic T, Perovic J, Purenovic M, Blagojevic S, Nikolic R, Andjelkovic D, Bojic A. A Direct Potentiometric Titration Study of the Dissociation of Humic Acid with Selectively Blocked Functional Groups. Eclética Química. 2006; 31(30):1-9.

[4] Masini JC, Abate G, Lima EC, Hahn LC, Nakamura MS, Lichtig J, Nagatomy HR. Comparison of Methodologies for Determination of Carboxylic and Phenolic Groups in Humic Acids. Anal. Chim. Acta. 1998; 364:223-233.

[5] Riggle J, von Wandruska R. Condumetric Characterization of Dissolved Humic Materials. Talanta. 2002; 57:519-526

[6] Engebretson R, von Wandruszka R. The Effect of Molecular Size on Humic Acid Associations, Org. Geochem. 1997; 26:59-767.

[7] Patterson HH, Cronan CS, Lakshman S, Plankey BJ, Taylor TA. Comparison of Soil Fulvic Acids Using Synchronous Scan Fluorescence Spectroscopy, FTIR, Titration and Metal Complexation Kinetics. Sci. Total Environ. 1992; 113:179-196.

[8] Miano TM, Senesi N. Synchronous Excitation Flurescence Spectroscopy Applied to Soil Humic Substance Chemistry. Sci. Total Environ. 1992; 118:41-51.

[9] Kumke MU, Eider S, Krüger T. Fluorescence Quenching and Luminescence Sensitization in Complexes of Tb^{3+} and Eu^{3+} with Humic Substances. Environ. Sci. Technol. 2005; 39:9528-9533.

[10] Kumke MU, Frimmel FH, Ariese F, Gooijer C. Fluorescence of Humic Acids (HA) and Pyrene-HA Complexes at Ultralow Temperatures. Environ. Sci. Technol. 2000; 34:3818-3823.

[11] Cory RM, McKight DM. Fluorescence Spectroscopy Reveals Ubiquitous Presence of Oxidized and Reduced Quinones in Dissolved Organic Matter. Environ. Sci. Technol. 2005; 39:8142-8149.

[12] Dong D, Winnik M. The py Scale of Solvent Polarities. Solvent Effects on the Vibronic Fine Structure of Pyrene Fluorescence and Empirical Correlations with E_T and Y values. Photochem. Photobiol. 1982; 35:17–21.

[13] Product Literature, Coulter N4 Plus Sub micron Particle Sizer, Coulter Corporation, Miami, FL, USA.

[14] Prevedouros K, Cousins IT, Buck RC, Korzeniowski SH. Sources, Fate and Transport of Perfluorocarboxylates. Environ. Sci. Technol. 2006; 40(1):32-44.

Chapter Three

The Effects of Conformational Changes on the Native Fluorescence of Aqueous Humic Materials

American Chemical Science Journal, 4(3): 326-336, 2014

3.1 Abstract

Aims: To elucidate the effect of induced conformational changes on the native fluorescence of aqueous humic materials.

Study Design: The conformation of dissolved humates was changed by adjustment of a variety of environmental factors and the resulting fluorescence emission, excited at 240nm was monitored in the 300-465nm range.

Place and Duration of Study: Department of Chemistry, University of Idaho, Moscow, ID, USA; April to August, 2012

Methodology: The fluorescence spectra of a number of humic and fulvic acids in different solution environments were measured with a photon counting fluorimeter. Attention was focused on the emission range centered on 400 nm and the intensity of the peak observed in this region was interpreted in terms of conformational changes.

Results: The addition of a multivalent cations produced distinct changes in the native fluorescence of dissolved humic materials that had otherwise broad and featureless emission spectra. A series of divalent cations were found to produce these emission changes. Microaggregation brought about by alternative causes, such as changes in pH, concentration, and solvent, produced similar outcomes. Chain length and rigidity of the humic polyanions also had significant effects.

Conclusion: The appearance and variation of a 400-nm emission peak was rationalized by invoking the formation of pseudomicellar structures that incorporated the emitting entity and provided limited access to water.

3.2 Introduction

Humic substances, the decay products of the total biota in the environment, tend to have highly aromatic cores containing numerous fluorophores [1]. The abundance and similarity of these entities lead to broad, relatively featureless spectra that are of limited analytical utility. For this reason, fluorimetric investigations of humates involving strongly emitting probes are often more fruitful than those relying on native emissions [2]. One technique that does use the native fluorescence to good effect is total fluorescence spectroscopies in which excitation emission matrices are generated that provide fingerprint-like identification for mixtures of fluorophores [3].

Close inspection of single-scan native fluorescence of humates, however, reveals that certain spectral features of aqueous humates are related in interesting ways to the solution conditions of the humic biopolymers. These responses are based on conformational changes in the materials and aggregates that form as a consequence of environmental influences [4]. The present communication deals with emission changes that occur because of such conformational variations.

The conformations of humic polyanions in aqueous solution have been studied extensively [4]. It is generally agreed that the highly diverse humic solutes progressively aggregate in response to solution parameters such as pH, ionic strength and presence of multiply charged cations, temperature, and concentration [5]. One of the more interesting features of this process is the formation of humic pseudomicelles [6,7], which can be visualized as microscopic units that, while lacking the ordered structure of a “regular” surfactant micelle, do provide an internal microenvironment that can accommodate hy-

drophobic co-solutes. The presence of di- and trivalent cations in solution is especially favorable for the formation of humic pseudomicelles, since these ions can bind to functional groups (especially carboxylates) on different parts of the humic structure, thereby connecting them into a coherent entity. It has been shown that this process is accompanied by a reduction in particle size [8].

3.3 Experimental Details

3.3.1 Chemicals

All chemicals were of analytical grade. $MgCl_2$ and NaCl was purchased from Fisher Scientific. $[(CH_3)_3\,NCH_2CH_2N(CH_3)_3]^{2+}$ ("N2"), europium chloride, and holmium chloride were purchased from Sigma Aldrich. $Sr(NO_3)_2$, $CaCl_2$, $Tb(NO_3)_3$, and $La(Cl_3\,)H_2O$ were obtained from J.T. Baker Chemical Co. EM Industries, Pfaltz and Bauer, and Strem Chemicals, respectively. All reagents were used as received. Standard humic and fulvic acids were purchased from the International Humic Substances Society (IHSS, St. Paul MN 55108) and used as received.

3.3.2 Isolation and Dissolution of Humates

Latah Co Silt Loam Humic Acid (LSLHA) was isolated from Latah Co Silt Loam (Argiaquic Xeric Argialbolls) according to the procedure provided by IHSS [9] which involves two cycles of HCl treatment for the removal of acid-soluble material; extraction of the residue with 0.1M 328 NaOH; deashing with 0.1 M HCl/0.3M HF; purification by dialysis and isolation by freeze drying. Humic acid solutions were prepared in doubly distilled

water, treated with a Millipore Milli-Q Reagent water system to a resistivity of at least 16 MΩ cm. The material was brought into solution by adding a minimal amount of base (sodium or ammonium hydroxide) and subsequently adjusting the pH to the desired value with 0.01 M HCl. For humate solutions containing magnesium or other metals, the appropriate increments of a 5 µg/mL of the metal chloride was added to a 10 µg/mL solution of the humate.

3.3.3 Fluorescence

Fluorescent spectra was taken with a Fluorolog-3 fluorimeter (Horiba Jobin Yvon, Edison, NJ) with photon counting detection. The samples were excited at 240 nm and the emission spectra were collected in the 300-465nm range. Confirmation measurements were obtained with an SLM-Aminco 8100 Fluorescence Spectrophotometer (Urbana, IL).

3.4 Results and Discussion

The fluorescence emission spectrum of a 10µg/mL aqueous solution of LSLHA, excited at 245 nm, is shown in Fig. 3.1. The typical broad emission can be seen to increase gradually in intensity over the 300-465 nm range. The addition of Mg^{2+} to the solution gave rise to general intensity enhancement, as well as a distinct peak centered at 400 nm. Ca^{2+} and a series of divalent lanthanide ions produced similar effects, while monovalent cations such as Na^{+} did not – even at high concentrations. The lanthanides gave an additional spectral feature around 370 nm (not shown here), which can be ascribed to sensitized emission and will not be considered further.

It has been shown [10] that Mg^{2+} and other did and trivalent cations cause aqueous humates to undergo progressive intra- and intermolecular aggregation, in which the humic polyanions are drawn into structures that resemble surfactant micelles ("pseudomicelles"). It may be hypothesized that these configuration changes cause humic fluorophores – *e.g.* the one giving rise to the 400-nm peak – to be placed in a different, less polar, environment and therefore display different emission characteristics. The measurements described here were carried out to clarify this matter.

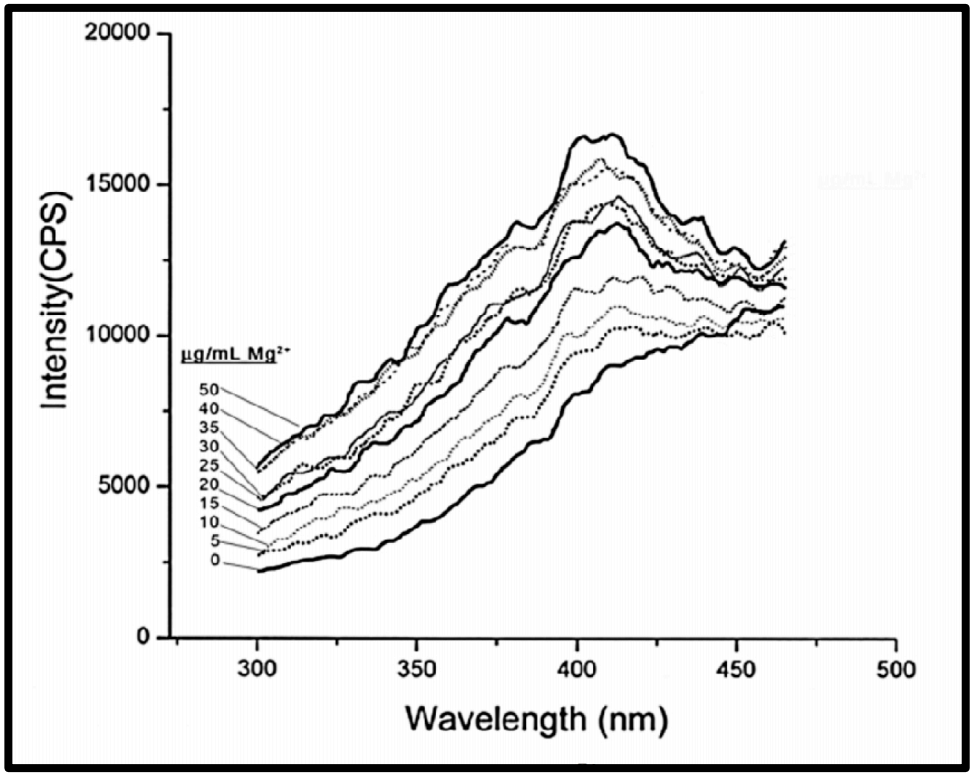

Figure 3.12. Effect of different concentrations of Mg^{2+} on the intrinsic fluorescence of LSLHA in the 300-465 nm range; ex 245nm; 10 µg/mL LSLHA

3.4.1 Effect of pH

The addition of multivalent cations is the most efficient, but not the only way to induce pseudomicelle formation in dissolved humates. A similar effect can be achieved by reducing the pH of a humic solution; thereby protonating the carboxylate groups of the polyanions [11]. Once these are neutralized sufficiently to minimize coulombic repulsion, the humic chains can fold to form microscopic aggregates with an internal environment that may allow the 400-nm emission peak to appear. The experimental evidence Fig. 3.2 supported this scenario. It can be seen that the telltale peak at around 400 nm became clearly visible at pH 2, lending further credence to the notion that the sequestration of humic fluorophores in the relatively nonpolar interior of the pseudomicelles gave rise to this emission.

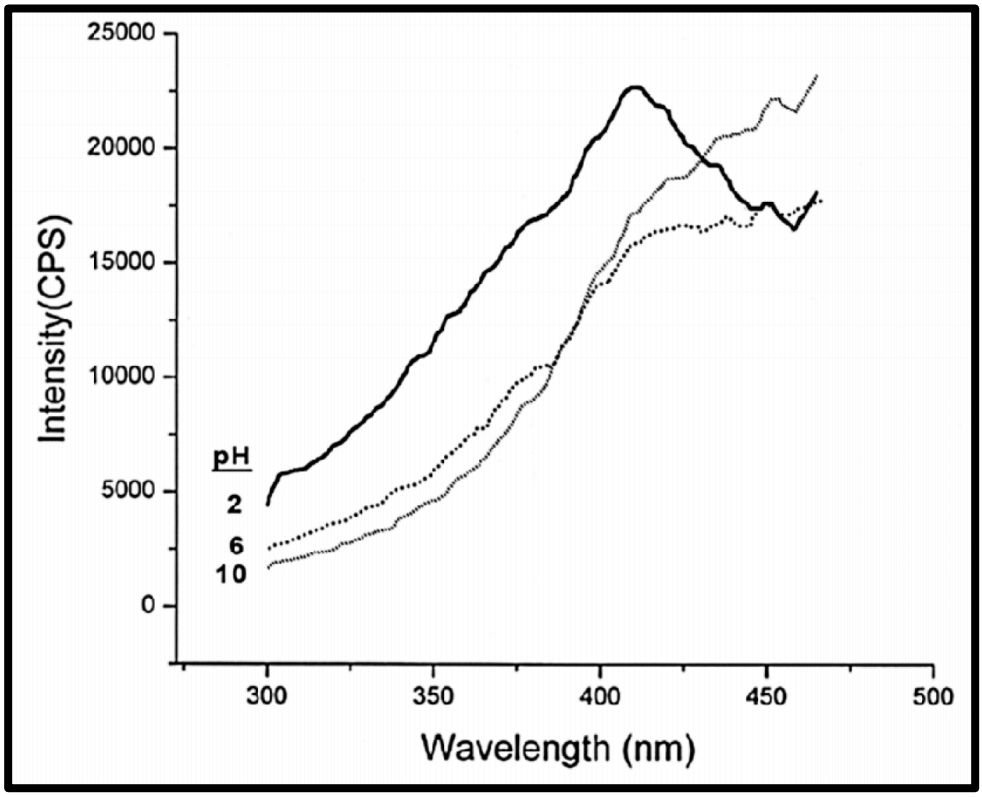

Figure 3.13. The effect of pH on the fluorescence of LSLHA (55 µg/mL; ex 245nm)

3.4.2 Solvent Polarity

In previous work involving humic solutions with an added fluorescent probe [12] it was noted that the sequestration of this probe within the pseudomicelles showed that it resided in a relatively nonaqueous microenvironment. In the present case, this apparent exclusion of water from the interior of the humic aggregate is also invoked to explain the 400-nm native emission of the humate. It therefore should be expected that the a priori use of a less polar solvent would have a similar effect. To this end, a series of 2-propanol – water mixtures were used as solvents for LSLHA, and the fluorescence characteristics of the humate were monitored in each case. The results in Fig. 3.3 showed that the 400-nm fluorescence intensities increased with decreasing water content. For reason of scale, the trace for 100% propanol is not shown: it did, in fact, give a peak intensity that was approximately 2.5-fold greater than that of the 80% 2-propanol solvent. These data bear out the contention that water quenches the 400-nm emission and that the exclusion of water from the fluorophore leads to the observed enhancement.

3.4.3 Effects of Molecular Size

Previous work has shown that the formation of humic pseudomicelles is influenced by the molecular sizes of the species involved [13,14]. It is understood that any assembly of humic material is by nature polydisperse, and can display a wide variation in average size. In cases where there is a preponderance of relatively large polymeric material, it should be expected that internal folding and pseudomicelle formation is more

likely to occur. With small pieces, on the other hand, folding ("internal aggregation") cannot happen to the same extent. It has been shown previously that humic materials of which the molecular size has been reduced by photolysis, do not sequester hydrophobic species in aqueous solution in the manner that larger humates do [15]. This was ascribed to the lack of pseudomicelle formation in the photolyzed material.

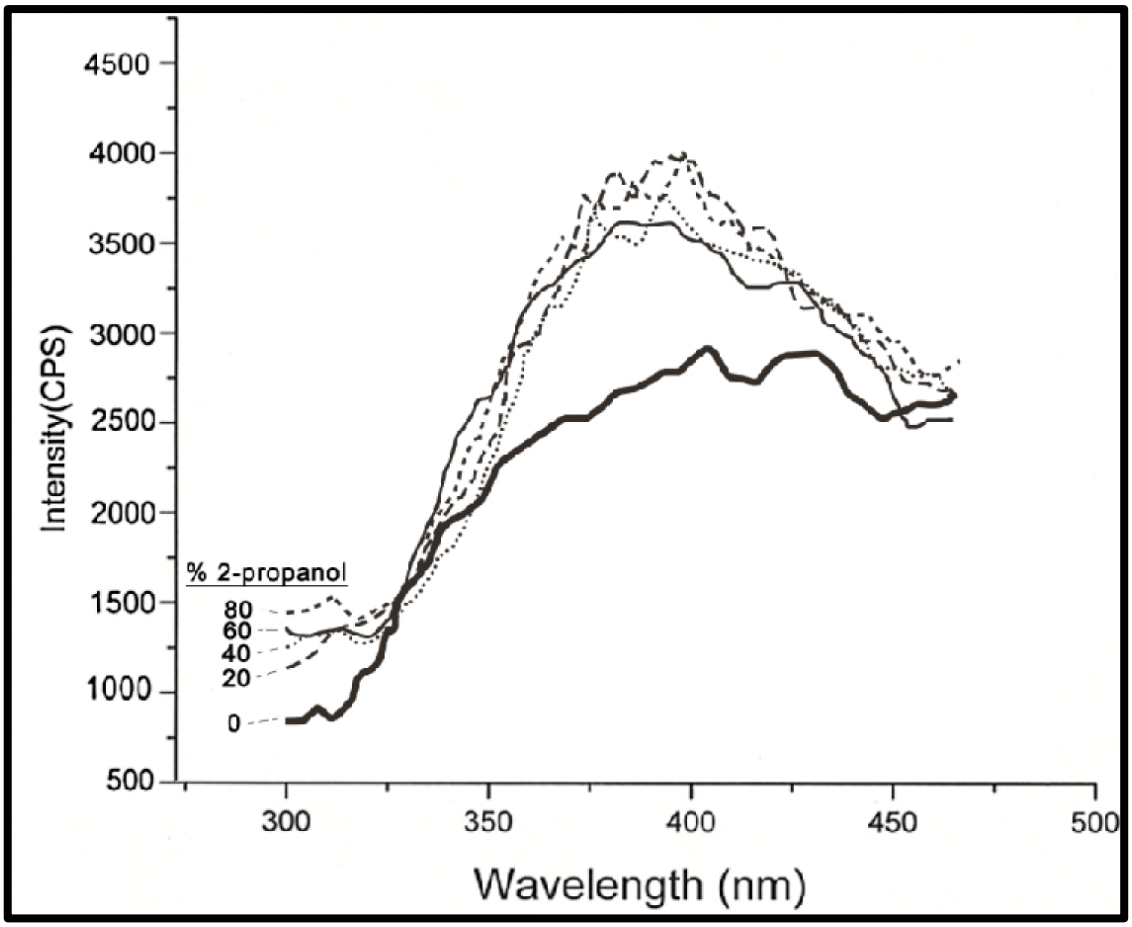

Figure 3.14. The effect of solvent composition on the 400-nm fluorescence of LSLHA

With this observation in mind, the fluorescence response of a photolyzed LSLHA solution to the addition of Mg^{2+} was monitored. Fig. 3.4 shows that the cation produced a general increase of intensity of the broad fluorescence band centered around 420 nm,

but that the telltale peak at 400 nm was not present. This fluorescence behavior was virtually identical to that of Minnesota Peat fulvic acid (not shown), which, being a fulvate, is a material of smaller molecular size that also lacks the ability to fold up into pseudomicellar structures. This observation adds yet more weight to the view that this conformational arrangement is the direct cause of the 400-nm peak.

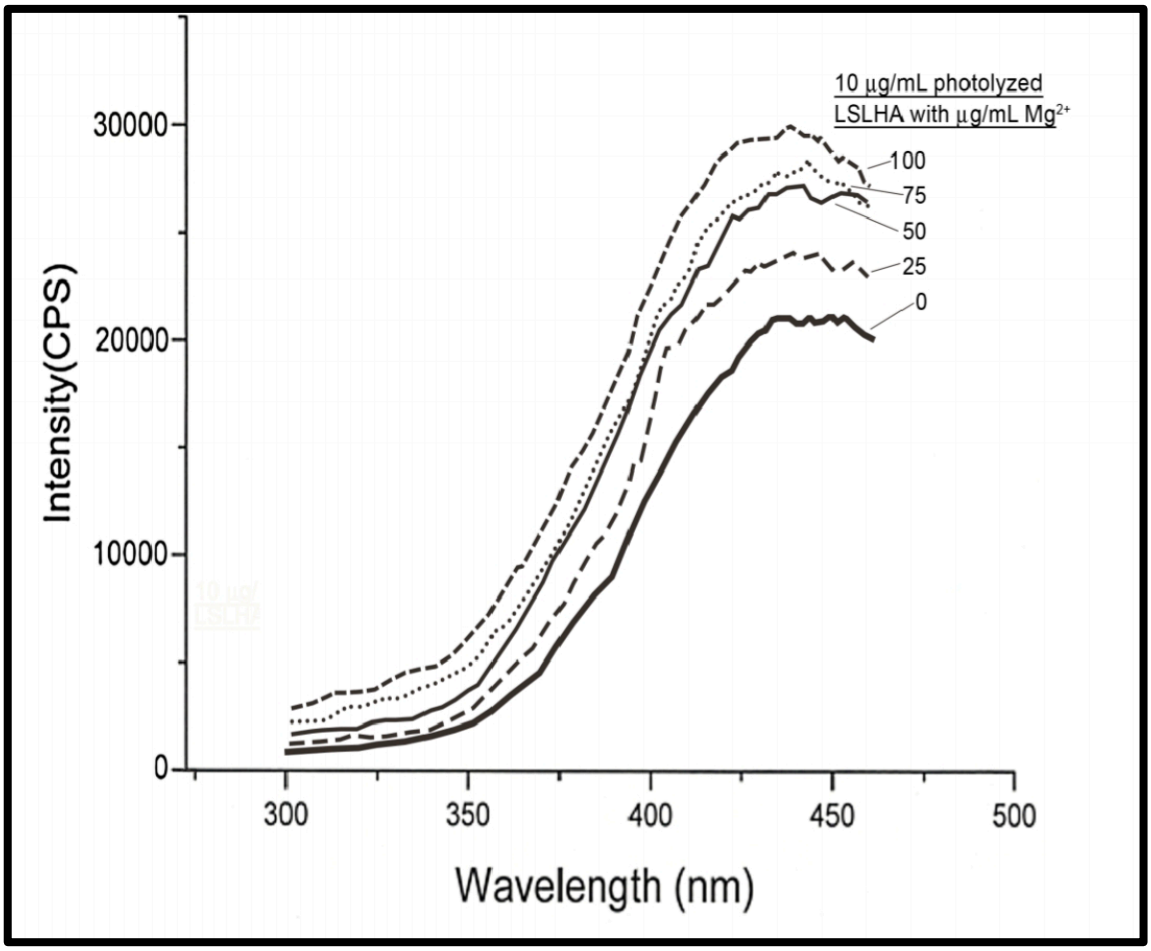

Figure 3.14. Fluorescence of photolyzed LSLHA at different Mg^{2+} concentrations

3.4.4 Effect of Concentration

It has been shown that increasing the concentration of aqueous humates also leads to progressive particle growth, including a pseudomicellar stage [7]. In view of this

phenomenon, the 400-nm emission peak was monitored as a function of humic concentration, and the results are shown in Fig. 3.5. While the development of the 400-nm peak was rather weak in this instance, it can be seen that the emission peak at this wavelength became more distinct at higher concentrations. I should be noted that the overall fluorescence intensity decreased with concentration from about 40 µg/mL onward because of an increasing inner filter effect.

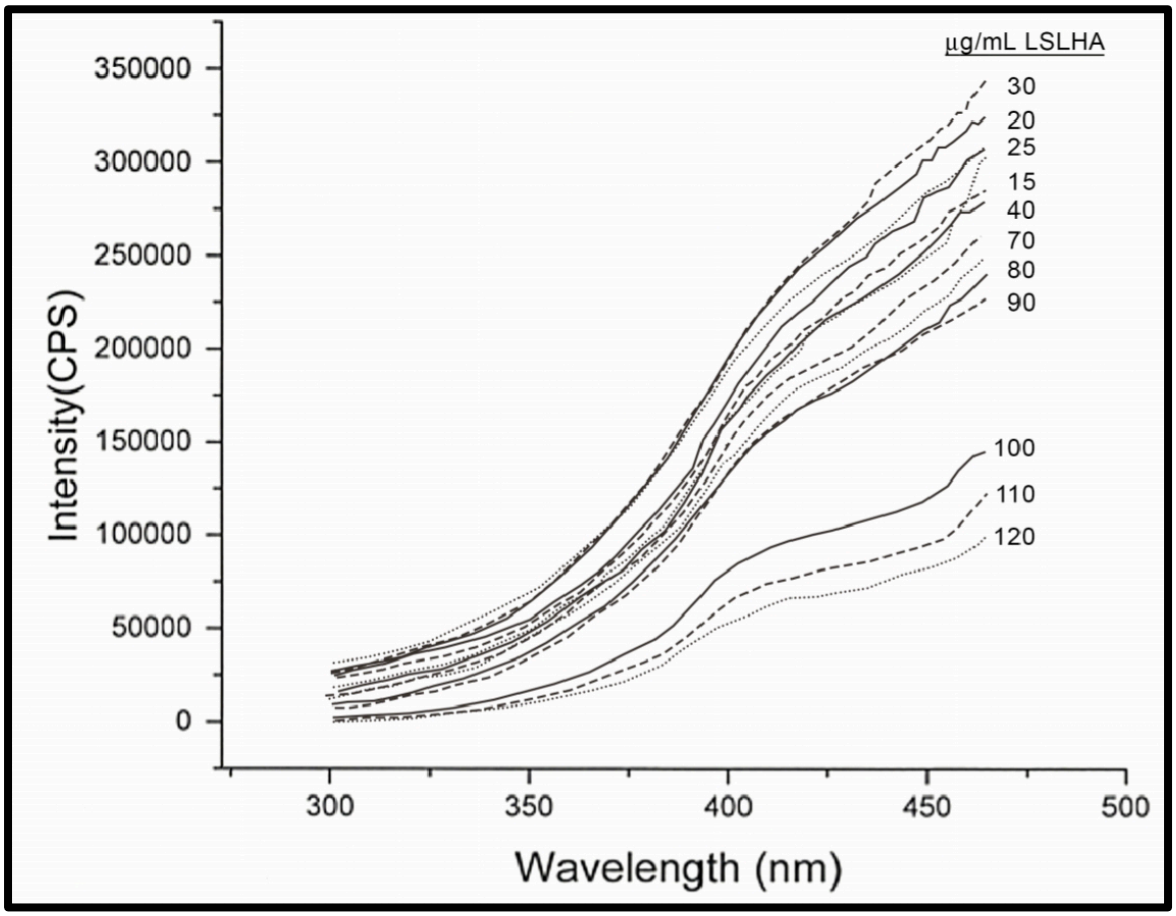

Figure 3.15. Family of emission spectra showing the effect of humate concentration on fluorescence

3.4.5 Large Cations

To evaluate the influence of cation size on humic fluorescence enhancement, a large organic cation, $[(CH_3)_3NCH_2CH_2N(CH_3)_3]^{2+}$ was used in place of Mg^{2+}. It was found that this large ion, at a concentration of 50 µg/mL, also enhanced the humic emission at 400 nm. This suggests that nonmetal divalent cations could undergo coulombic interactions with multiple anionic charges on the humic polymer. This, in turn, resulted in a similar pseudomicellar contraction as was observed with multivalent metal ions. In addition, the alkyl moiety of these large cations appeared to be accommodated within the humic structure, enhancing its micellar character.

3.4.6 Temperature

The emission intensity of fluorescent solutions generally decreases with temperature as the thermal motion of fluorophores increases non-radiative deactivation of the excited state [16]. Fig. 3.6 shows that this was the case with the 400-nm emission peak of an LSLHA solution treated with Mg^{2+}. It is interesting to note, however, that while the intensity decreases upon heating, the peak does not appear to lose its shape. This suggests that thermal agitation in the 30-60^{o} C temperature range, did not lead to significant disaggregation.

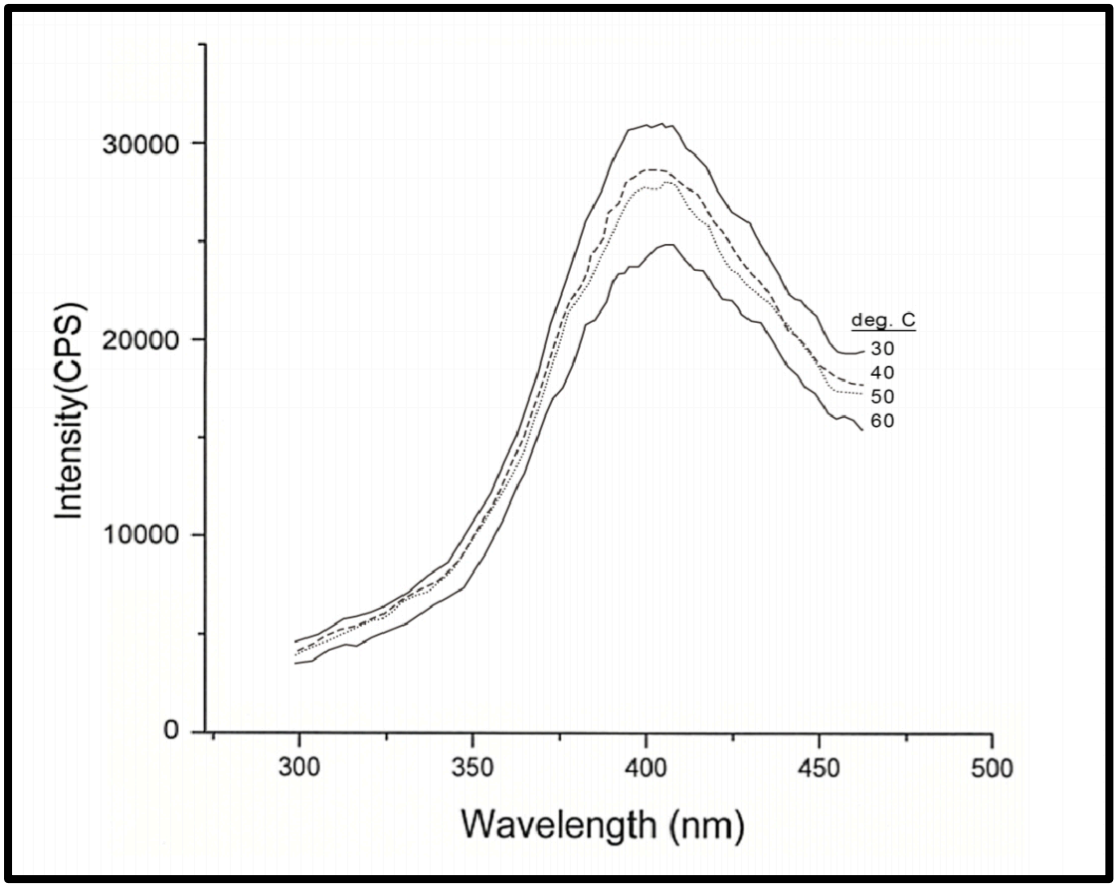

Figure 3.16. The effect of temperature on the 400-nm emission of LSLHA in the presence of Mg^{2+}

3.4.7 Different Humates

While the mechanism of humic pseudomicelle formation is not entirely understood, it is reasonable to assume that it, as suggested above, involves the folding of polymeric chains and the incorporation of smaller entities in micro aggregates of roughly micellar size [15]. In view of this, the flexibility of the humic chains should be a factor, since it influences their ability to fold and twist into the proper configuration. It is therefore instructive to compare the fluorescence behavior of LSLHA, which comprises relatively flexible polymer chains, with that of other humates with both similar and different structure. In this context, the fluorescence response of the IHSS standards Summit Hill

HA and Peat HA to Mg^{2+} was tested. These materials have aggregation properties similar to LSLHA [17] and it was found that the 400-nm emission peak also appeared when Mg^{2+} was added (spectra not shown). Leonardite humic acid (LHA), on the other hand, is a good example of a stiffer, less flexible, humate. Its quantitative ^{13}C NMR spectrum shown in ref [18]. Contains a large aromatic peak at 127 ppm, indicating that it is more aromatic and coal-like in nature than other humates. This structure, containing multiple fused rings, cannot be deformed easily. The spectra shown in Fig. 3.7 are consistent with these structural constraints. The 400-nm emission peak could be generated, but to get a comparable effect with LHA it took about ten times as much Mg^{2+} as it did with LSLHA. These points to less easy intra-molecular rearrangements of the stiffer LHA polyanions, requiring more cationic anchors to create pseudomicellar aggregates.

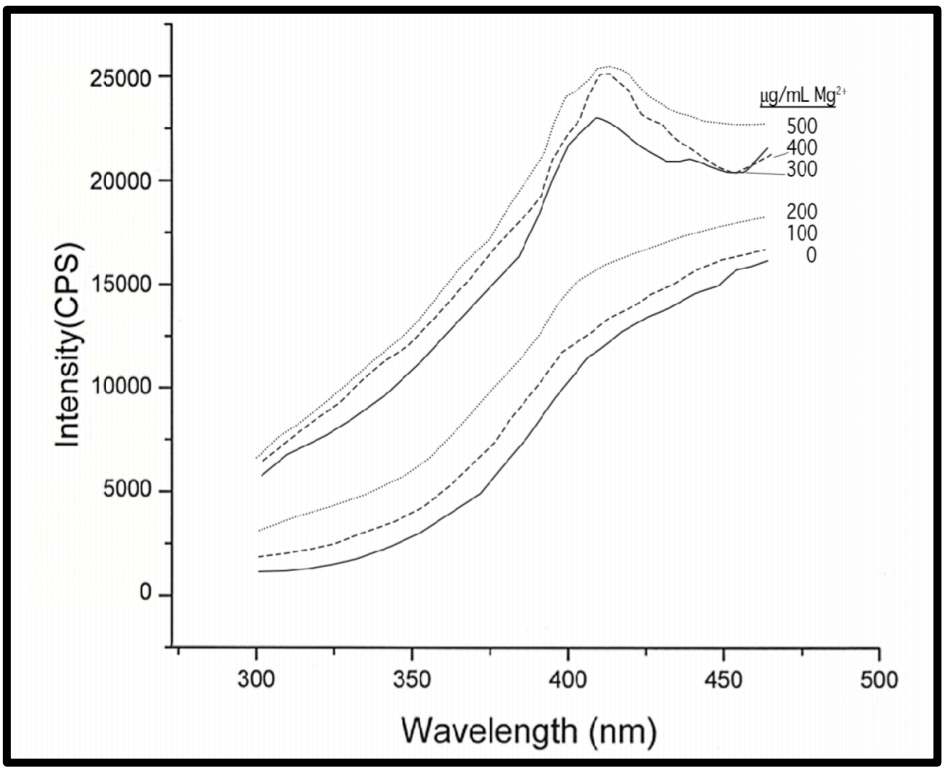

Figure 3.17. Fluorescence spectra of LHA at different Mg^{2+} concentrations

3.4.8 Micellar Solutions

A nonpolar, relatively water free, microenvironment in which the 400-nm humic emission peak potentially could be observed can also be created by using a micellar solution of a surfactant [19] and introducing small amounts of LSLHA to it. Incorporation of the humate in the micelles should expose it to a relatively dry environment favorable to the appearance of the 400-nm peak.

The experiment was carried out with a 1.0 mM solution of cetyltrimethyl ammonium bromide (CTAB), a cationic surfactant with a critical micelle concentration of 0.92 mM [20]. Small amounts of LSLHA were added drop wise in increments of approximately 0.3 µg. The results are shown in Fig. 3.8. From which it is clear that the 400-nm emission peak of LSLHA did indeed appear. This provides further confirmation for the necessity of the exclusion of water for this spectral feature to materialize.

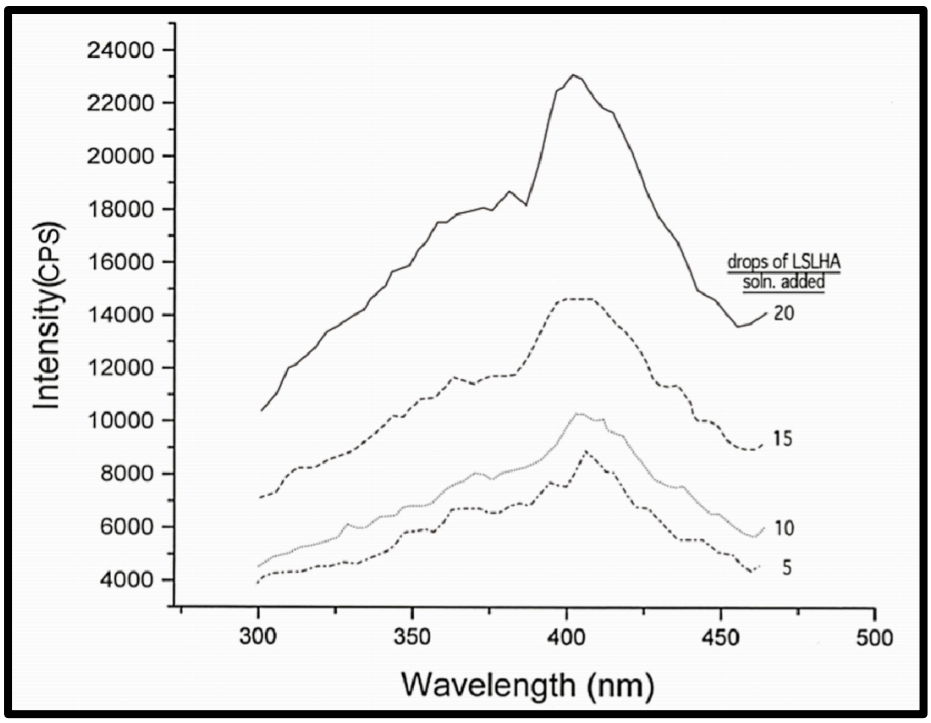

Figure 3.18. Fluorescence emission spectra of 50 mL of a 1.0 mM solution of CTAB with 110 µg/mL LSLHA added as indicated. Excitation wavelength 245 nm

3.5 Conclusions

The evidence presented here suggests that the fluorophore in LSLHA that is responsible for the emission peak at 400 nm is quenched by water, and that microaggregation of the aqueous humate can lead to significant exclusion of this quencher. This, in turn, is consistent with a pseudomicellar model of the humic material, in which the aggregates have a relatively polar exterior and a nonpolar interior. In aqueous solution, the 400-nm peak may be considered a marker for the formation of pseudomicelles. It was observed in different humates, and it may be cautiously proposed that it generally present in these materials. The nature of the fluorophore cannot be pinpointed at this time. Previous work [21] has shown that the ESR signal of quinonic entities that are common in humates change significantly when they aggregate under the influence of Mg^{2+} ions. The fluorescence characteristics of quinones, however, are quite different from the 245/400 nm ex/em wavelengths found here. The abundance of fluorophores in the humates make the unequivocal identification of the emitter responsible for the emission peak discussed here difficult, if not impossible.

3.6 References

[1] Patterson HH, Cronan CS, Lakshman S, Plankey BJ, Taylor TA. Comparison of soil fulvic acids using synchronous scan fluorescence spectroscopy, FTIR, titration and metal complexation kinetics. Sci. Total Environ. 1992; 113:179. Available: http://dx.doi.org/10.1016/0048-9697(92)90024-M

[2] Engebretson RR, von Wandruszka R. Effects of Humic Acid Purification on Interactions with Hydrophobic Organic Matter: Evidence from Fluorescence Behavior. Environ. Sci. Technol. 1999; 33:4299. Available: http://dx.doi.org/10.1021/es990386h

[3] Palmer NE, von Wandruszka R. The influence of aggregation on the redox chemistry of humic substances, Environ. Chem. 2009; 6:178. Available: http://dx.doi.org/10.1071/EN08081

[4] Shevchenko S M, Bailey GW, Akim LG. The Conformational Dynamics of Humic Polyanions in Model Organic and Organo-Mineral Aggregates. J. Mol. Structure: Theochem. 1999; 460:179. Available: http://dx.doi.org/10.1016/S0166-1280(98)00332-7

[5] Riggle J, von Wandruszka R. The Stability of U (VI) Complexes of Humates and Fulvates in Biphasic Systems. Ann. Environ. Sci. 2008; 2:1.

[6] Piccolo A, Nardi S, Concheri G. Micelle-like Conformation of Humic Substances as Revealed by Size Exclusion Chromatography. Chemosphere. 1996;33:595. Available: http://dx.doi.org/10.1016/0045-6535(96)00210-X

[7] von Wandruszka R. The Micellar Model of Humic Acid: Evidence from Pyrene Fluorescence Measurements. Soil Sci. 1998;163:921. Available: http://dx.doi.org/10.1097/00010694-199812000-00002

[8] Palmer N, von Wandruszka R. Size Dynamic light scattering measurements of particle Development in Aqueous Humic Materials, Fresenius J. Anal. Chem. 2001; 371:951-954.

[9] International Humic Substances Society. Product Literature. St. Paul, MN, January 25; 1985.

[10] von Wandruszka R, Ragle C, Engebretson R. The role of selected cations in the formation of pseudomicelles in aqueous humic acid. Talanta. 1997; 44:805. Available: http://dx.doi.org/10.1016/S0039-9140(96)02116-9

[11] Terashima M, Fukushima M, Tanaka S. Influence of pH on the Surface Activity of Humic Acid: Micelle-like Aggregate Formation and Interfacial Adsorption. Coll. Surf. A: Physiochem. Eng. Aspects. 2004; 247:77. Available: http://dx.doi.org/10.1016/j.colsurfa.2004.08.028

[12] Engebretson R, Amos T, von Wandruszka R. Quantitative Approach to Humic Acid Associations, Environ. Sci. Technol. 1996; 30:390. Available: http://dx.doi.org/10.1021/es950478g

[13] Chilom G, Bruns AS, Rice JA. Aggregation of Humic Acid in Solution: Contributions of Different Fractions. Org. Geochem. 2009; 40:455. Available: http://dx.doi.org/10.1016/j.orggeochem.2009.01.010

[14] Engebretson RR, von Wandruszka R. The Effect of Molecular Size on Humic Acid Associations. Org. Geochem. 1997; 26:759. Available: http://dx.doi.org/10.1016/S0146-6380(97)00057-0

[15] Engebretson RR, von Wandruszka R. Micro-organization in Dissolved Humic Acids, Environ. Sci. Technol. 1994; 28:19-34.
Available: http://dx.doi.org/10.1021/es00060a026

[16] Guilbault G. General Aspects of Luminescence Spectroscopy, in Practical Fluorescence, 2nd ed. (Ed. G. Guilbault). Marcel Dekker: New York. 1990; 28.

[17] Yates LM, Engebretson RR, Haakenson TM, von Wandruszka R. Immobilization of Aqueous Pyrene by Dissolved Humic Acid, Anal. Chim Acta. 1997; 356:295.
Available: http://dx.doi.org/10.1016/S0003-2670(97)00503-5

[18] Thorn KA, Folan DW, Mac Carthy P. Characterization of the International Humic Substances Society standard and reference fulvic and humic acids by solution state carbon-13 (13 C) and hydrogen-1 (1 H) nuclear magnetic resonance spectrometry, Water-Resources Investigations Report 89-4196, U.S. Geological Survey, Denver, CO 80225; 1989.

[19] Meyers D. Surfactant Science and Technology. VCH, New York. 1988, 93.

[20] Sigma-Aldrich product information for Hexadecyltrimethylammonium bromide.
Available:
http://www.sigmaaldrich.com/catalog/product/fluka/52367?lang=en&region= US

[21] Bakajova B, von Wandruszka R. Radical stabilization in dissolved humates, Open J. Phys. Chem. 2011; 1(3). Available: http://dx.doi.org/55.10.4236/ojpc.2011.13008

Chapter Four

Temperature Induced Aggregation and Clouding in Humic Acid Solutions

Adv. Environ. Chem., vol. 2015, ID 543614, 6 pages (2015)
http://dx.doi.org/10.1155/2015/543614

4.1 Abstract

Humic acids in aqueous solution demonstrate inverse temperature-solubility relationships when solution conditions are manipulated to reduce coulombic repulsion among the humic polyanions. These effects were followed by dynamic light scattering (DLS) measurements of the resulting aggregates, as well as the addition of a polarity sensitive fluorescent probe (pyrene). The humic solutions could be primed for temperature induced clouding by carefully lowering the pH to a point where hydration effects became dominant. The exact value of the cloud point (CP) was a function of both pH and humate concentration. The CPs mostly lay in the range 50–90^{o} C, but DLS showed that temperature induced aggregation proceeded from approximately 30^{o} C onward. Similar effects could be achieved by adding multivalent cations at concentrations below those, which cause spontaneous precipitation. The declouding of clouded humate solutions could be affected by lowering the temperature combined with mechanical agitation to disentangle the humic polymers.

4.2 Introduction

Humic substances (HS) are the decay products of the total biota in the environment. They are grouped into three operationally defined categories: fulvic acid (FA), soluble at all pHs; humic acid (HA), soluble at pH > 2 ; and humin, insoluble at any pH. HA and FA are environmentally the most important components, HA being the most abundant. They exist in both aquatic and terrestrial environments and interact extensively with other soil and water constituents. They are generally classified as natural polyanions with approximate molecular weight ranges of 500 –2000 Da for FA and 2000 –20 ,000 Da for HA. In view of these broad size ranges, a high degree of polydispersity exists in aqueous solutions of humic materials [1]. They are mildly acidic, primarily due to an abundance of carboxylic groups [2].

Dissolved HA will aggregate and precipitate when certain conditions are imposed:

(i) The pH is lowered below 2, causing the protonation of acidic groups and resulting in reduced coulombic repulsion between the humic species.

(ii) Multivalent cations such as Mg^{2+}, Ca^{2+}, or Sm^{3+} that have the ability to form intra- and intermolecular ionic links between anionic (chiefly carboxyl) groups on the humates are added.

(iii) The ionic strength is raised sufficiently to result in a salting-out effect. Under these circumstances, the negative charges on the humic polyanions are shielded by the ionic content of the solution and coulombic

repulsion among the humates is reduced. This leads to the formation of aggregates.

It has been observed previously [3] that aqueous HA solutions, not unlike those of nonionic surfactants, can undergo temperature induced clouding (TIC). This is a manifestation of an inverse temperature-solubility relationship, in which the heating of the solution to a temperature known as the cloud point (CP) results in a cloudy appearance and eventually macroscopic phase separation. It is generally held that TIC in surfactant solutions is primarily due to the decrease of the relative permittivity, ε_r (a.k.a. dielectric constant) of water with temperature, which leads to reduced hydration of the hydrophilic portions of the molecules and hence to their aggregation. The value of ε_r for water at 20° C is 80.1 , while at 60° C it is 66.8 [4].

TIC is mostly encountered in nonionic surfactant solutions. Aqueous HA, at circum-neutral pH, is significantly ionic and does not display inverse solubility behavior. However, if one of the three conditions enumerated above is brought to bear—short of causing immediate precipitation— the solution conditions can be “tuned” to create a system that undergoes TIC. The likely cause of this is the partial suppression of the ionic character of HA, which makes effective hydration of the polar (but nonionic) portions of the molecules a more stringent prerequisite for solubility.

The work described in this communication focused on the details of TIC in aqueous solutions of humates, with emphasis on the solution conditions that promote the phenomenon. The bulk of the investigation was done with Latahco silt-loam humic acid

(LSLHA), which has been shown to be an effective surfactant [5].

4.3 Experimental Section

4.3.1 Reagents and Solutions

Pyrene was obtained from Aldrich and purified by cold finger sublimation. Perylene was obtained from Arcos Organics. The humic materials used were both purchased commercially and isolated from a local soil. The former were obtained from the International Humic Substances Society (IHSS, 1991 Upper Buford Circle, Rm 439, St. Paul, USA) and included the following: Leonardite Humic Acid Standard (LHA), Soil Humic Acid Standard (SHA), Summit Hill Soil Humic Acid Reference (SHHA), and Minnesota Peat Fulvic Acid Reference (MPFA). Latahco silt-loam HA (LSLHA) was isolated in the laboratory from Latahco silt-loam (Argiaquic Xeric Argialbolls) according to the International Humic Substances Society (IHSS) procedure published on January 25, 1985. Humic solutions were prepared with doubly deionized water treated with a 0 .22 µm Millipore filter system. Dissolution was affected by the drop-wise addition of a minimal amount of a 30% ammonium hydroxide solution. Reagent grade magnesium chloride hexahydrate was obtained from Baker, sodium chloride from Macron, samarium chloride from Aldrich, and hydrochloric acid from Fisher.

4.3.2 Fluorescence Measurements

Fluorescence emission and excitation measurements were obtained with a Fluorolog-3 fluorimeter manufactured by Horiba JobinYvon. Confirmation measure-

ments were carried out with SLM Aminco 8100 and Hitachi U-4500 fluorescence spectrophotometers. For the determination of pyrene I_1/I_3 emission ratios, the solutions were excited at 240 nm and the emissions were measured at 372 nm (I_1) and 384 nm (I_3). An expanded range thermometer purchased from Fisher Scientific was used to measure the temperature of the solution and confirm thermal equilibration before the fluorescent measurements were taken. Multiple spectra were taken to confirm results.

4.3.3 Particle Sizing

The size of humic aggregates was determined by dynamic light scattering measurements, using a Coulter N4 Plus Submicron Particle Sizer. The instrument employed a He-Ne laser light source (632.8 nm), and the scattering intensity was measured at a 90^o angle. Measurements were carried out in the unimodal mode [6]. Temperature control was implemented through an internal electronic- Peltier heater/cooler with a precision of $\pm 0.2^o$ C at 25^o C. Temperatures ranged from 20^o C to 60^o C. Duplicate measurements of 300 s were taken to confirm results. 2.4. pKa. The pKa of LSLHA was determined by titrating 125 mL of 40 mg/L LSLHA with a carbonate-free 0.04 M NaOH solution, held at 22°C under nitrogen [7]. After dissolution of the HA sample with a minimal amount of base, the solution was acidified to pH 2.5 with HCl prior to titration. The titration was performed with a Schott Titronic automated titrator, set to dispense 0 .10 mL of titrant every 60 s, and a Vernier glass combination electrode.

4.4 Results and Discussion

4.4.1 pH Adjustment

As noted in the Introduction, the occurrence of TIC in humic solutions is predicated on a reduction of the ionic character of the solute, allowing it to aggregate when the temperature is raised. In our first series of experiments, this was achieved by lowering the pH to 2.5, which converted the humate to a form akin to a nonionic surfactant. At 20^{o} C, a 40 mg/L LSLHA solution did not cloud under these conditions, but when the temperature was increased, visible clouding occurred. The solution conditions under which the effect was observed are summarized in Table 1.

Table 4.1. Cloud points (^{o}C) of LSLHA solutions at different pH

pH	Concentration (mg/L)			
	40	60	80	100
2.5	56	51	50	46
3.0	n.o.*	87	74	75
3.5	n.o.	n.o.	95	90

Not observed*

The data shows that the cloud point decreased with increasing concentration and decreasing pH, with a pH of 3.5 being an effective cut-off value above which no TIC occurred. In terms of the value of the pKa of LSLHA, determined [8] to be 3.89, lowering the pH to 2.5 for solubility reversal corresponds to the carboxyl groups of the material being approximately 96% protonated.

In view of the expectation that visible clouding would be preceded by progressive particle growth, the effect was quantitatively followed through fluorescent probe and dynamic light scattering measurements.

4.4.2. I_1/I_3 Ratio

Pyrene is a fluorophore that has been proven suitable as a probe for the study of aggregation in humic solutes [8]. The ratio of the first and third vibronic peaks in the pyrene emission spectrum (I_1/I_3 ratio) is widely used to assess the polarity of the environment of the fluorophore [9-11]. When pyrene is sequestered by humic aggregates, in a manner analogous to micellization by synthetic surfactants, the I_1/I_3 ratio tends to decrease as a result of the reduced polarity experienced by the probe. In this manner, the ratio can be used to track the aggregation processes. Fig. 4.1 shows the variation of the I_1/I_3 ratio with temperature leading up to the cloudpoint.

Two counteracting processes were in effect when the temperature of the primed humic solutions was increased: (i) thermal agitation (which tends to disrupt the aggregates) and (ii) dehydration (which promotes aggregate formation). The data in Fig. 4.1 suggest that in the 20 –35° C range the two effects largely canceled each other, resulting in a relatively flat curve. Beyond 35° C, the I_1/I_3 ratio monotonically decreased, indicating that pyrene experienced an increasingly nonpolar environment. No such effect was observed with an aqueous pyrene solution in the absence of HA, so it can be concluded that temperature-induced aggregation (TIA) of humate progressively took place as the solution was heated, culminating in TIC at 70° C.

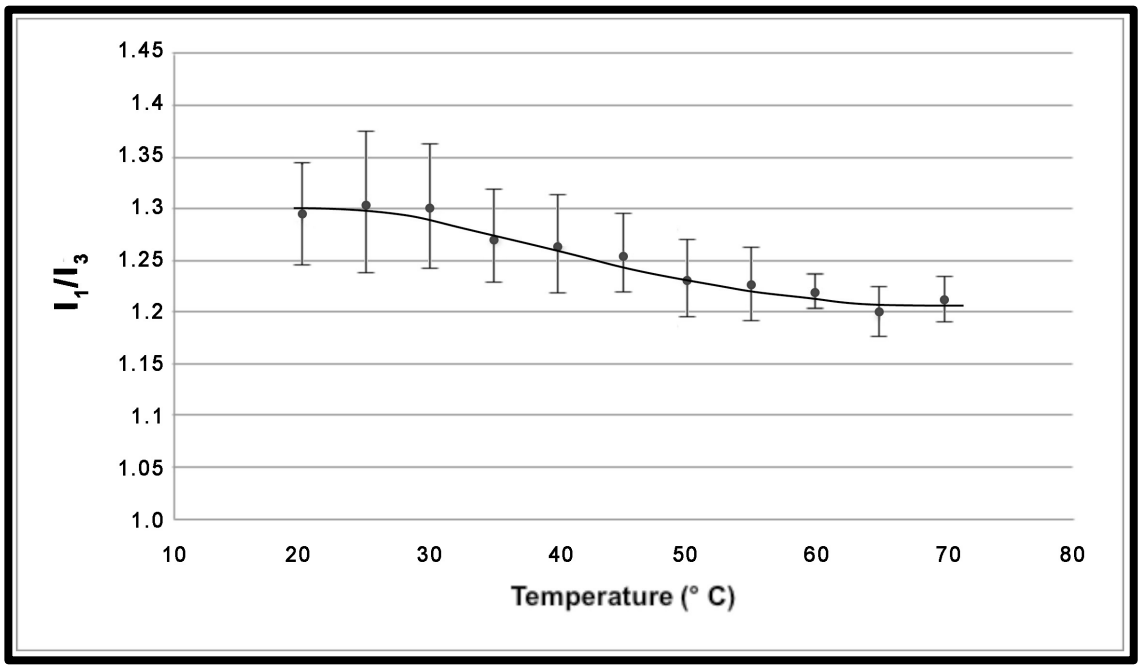

Figure 4.19. Variation of pyrene I_1/I_3 ratio with temperature in 40 mg/L LSLHA at pH 2.5

Direct evidence of TIA of dissolved humate was provided by dynamic light scattering measurements of an LSLHA solution at pH 2.5. The steady increase of average particle size with temperature shown in Fig. 4.2 is consistent with I_1/I_3 ratio changes discussed above. It is important to note that the data in Fig. 4.2 were obtained with a solution that did not contain pyrene, that is, a nonpolar solute that may act as a nucleation center for amphiphilic humates [2]. The particle growth observed under these circumstances lends further credence to the principal role of temperature in the aggregation process.

A further interesting observation was made when the particle sizes in a circumneutral solution of LSLHA containing pyrene were measured at a series of increasing temperatures.

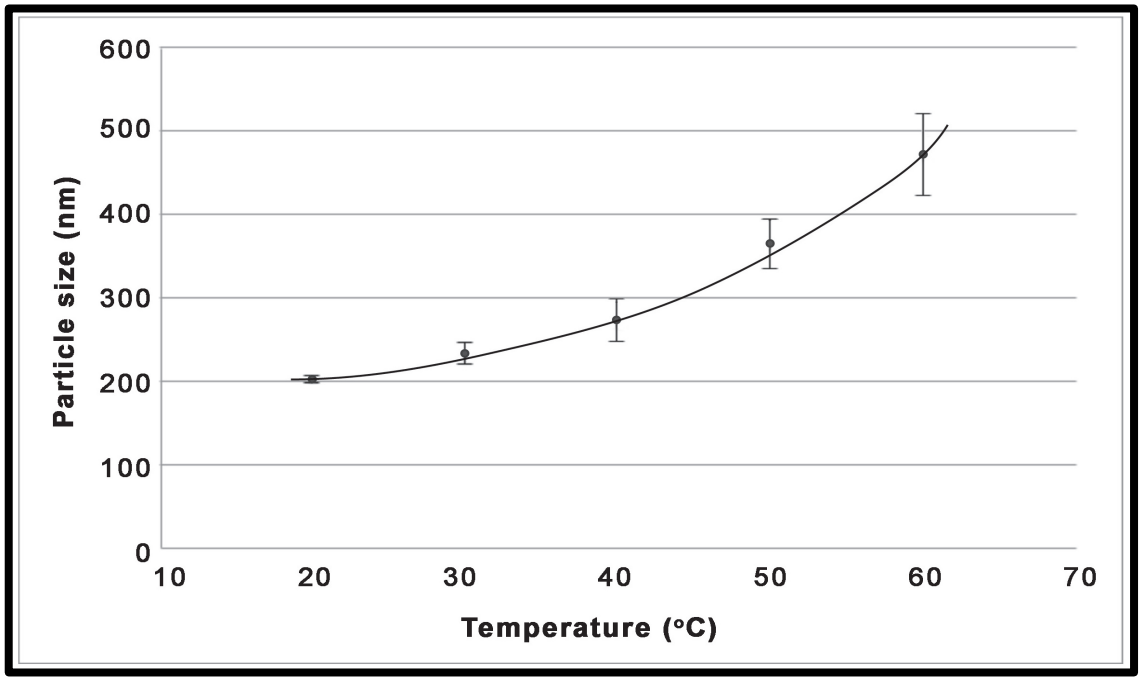

Figure 4.20. Variation of particle size with temperature in 40 mg/LSLHA at pH 2.5

Fig. 4.3 shows that particle sizes in this solution, in which the humate was not significantly protonated and no temperature-induced effects should be expected, decreased with temperature. This can be rationalized by considering that a similar solution without pyrene would have a particle size around 200 nm, which is invariant with temperature. The presence of pyrene led to a small degree of hydrophobic association with humate, even in the absence of significant aggregation of the latter, giving rise to slightly increased particle sizes (ca. 275 nm). Upon heating, however, these weak aggregates were thermally disrupted, and the particle sizes decreased.

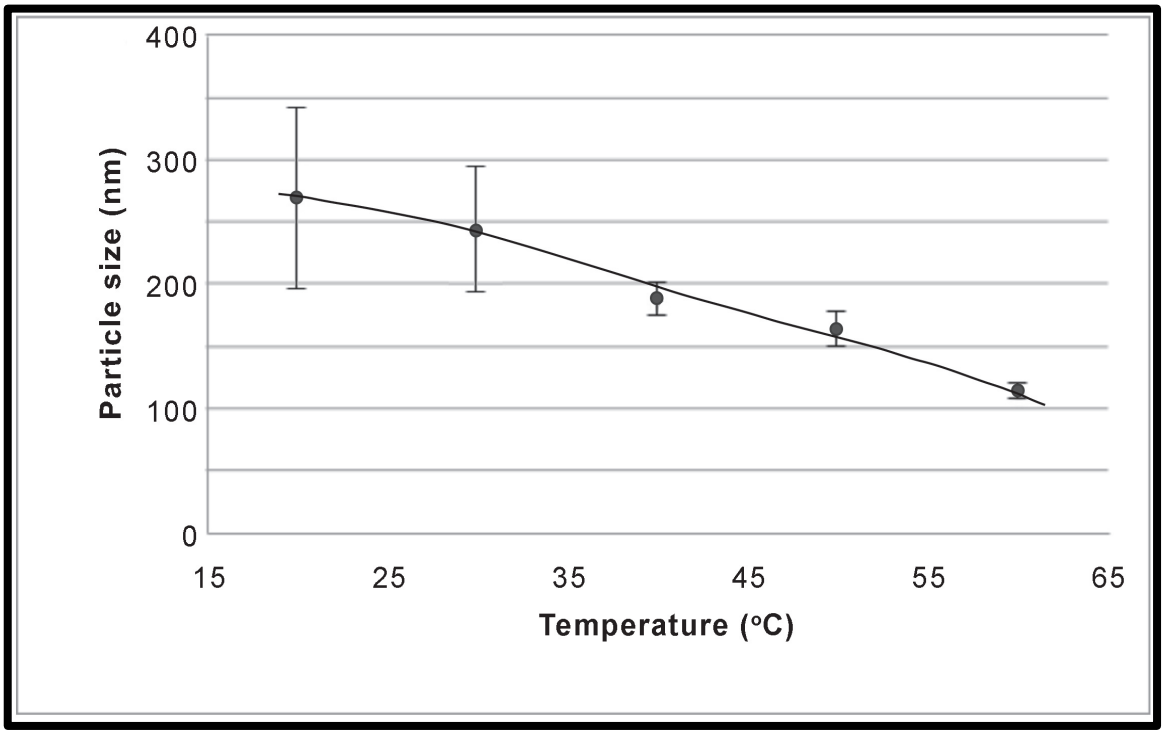

Figure 4.21. Variation of particle size of 40mg/L LSLHA and 10^{-6} M pyrene (pH 7.5)

4.4.3 Effects of Cations

Raising the ionic strength of HA solutions can lead to aggregation and precipitation of the solutes. At ionic strengths below those that lead to complete salting out at room temperature, TIC/TIA effects can be observed. Monovalent cations are less effective than di- and trivalent ones, and in the case of NaCl, TIC took place at 70^{o} C in 60 mg/L LSLHA only when the salt was added in excess of 1 M. With a more modest 0.008 M NaCl concentration (twice that of the $MgCl_2$ solutions, giving the same cationic strength) DLS particle sizing in a LSLHA solution showed no aggregation effects at temperatures up to 60° C. In fact, as shown in Fig. 4.4, a very slight decrease in particle size with temperatures was found. This size reduction, which was not observed in HA solu-

tions without salt, can be attributed to the thermal disruption of electrolyte shielding [12] of the anionic charges on the humates. At low salt concentrations, this shielding process allowed for slight aggregation of the humic polymers [13], producing relatively small and fragile particles that disintegrated when thermally agitated.

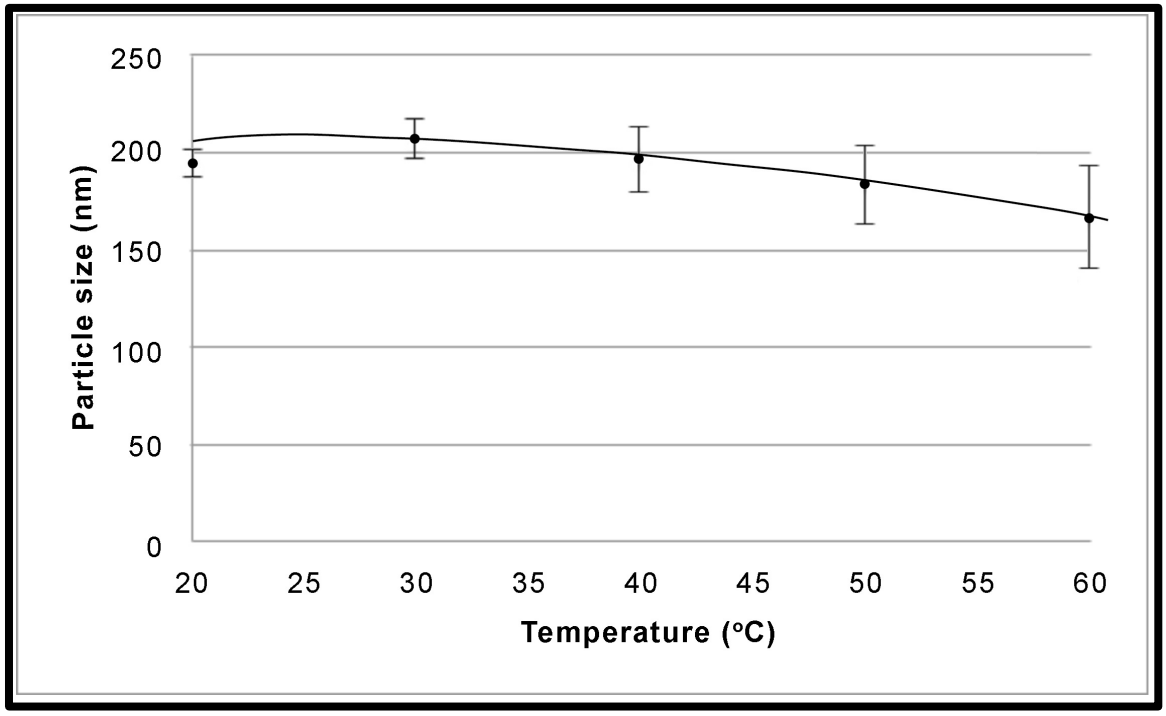

Figure 4.22. Variation of particle size with temperature of 40 mg/L LSLHA and 0.008 M NaCl (pH 7.5)

In the presence of relatively low concentrations of $MgCl_2$, the intra- and intermolecular crosslinking of humic entities byMg^{2+} effectively primed the system for TIC. Table 2 shows a summary of the cloud points of different concentrations of LSLHA in 0.004 M aqueous $MgCl_2$ solutions. For comparison, values of IHSS humic and fulvic acids are also shown.

Table 4.2. Cloud points (^{o}C) of humic materials in 0.004M $MgCl_2$ solutions.

HA	40mg/L	60mg/L	80mg/L	100mg/L
LSLHA	54	50	51	50
Leonardite HA (LHA)	75	67	55	57
Soil HA (SHA)	69	65	65	45
Summit Hill HA (SHHA)	n.o.*	n.o.	n.o.	n.o.
Minnesota Peat FA (MPFA)	n.o.	n.o	n.o.	n.o.

It can be seen that LSLHA clouded at relatively low temperatures and that the cloud points were similar over the concentration range. More varied and higher cloud points were found with LHA and SHA, while, interestingly, SHHA and MPFA did not cloud at all. It is not immediately clear why the latter two could not be primed to behave as nonionic surfactants. The reason may lie in the fact that these are aquatic materials with a possibly less pronounced amphiphilic nature.

Figs. 4.5 and 4.6 show the respective temperature responses of particle size and the pyrene I_1/I_3 ratio in LSLHA solutions containing $MgCl_2$. Both the lowering of the pH and the addition of Mg^{2+} rendered the LSLHA solute sufficiently nonionic to undergo TIA/TIC. The CP was lower in the latter case, showing that the intra- and intermolecular crosslinking caused by divalent cation were more effective in readying the system for temperature induced effects. LSLHA has a relatively flexible backbone allowing the Mg^{2+} ions to “pull together” and crosslink dispersed portions of the humic polyanions, thereby forming a pseudo-micellar particle [14].

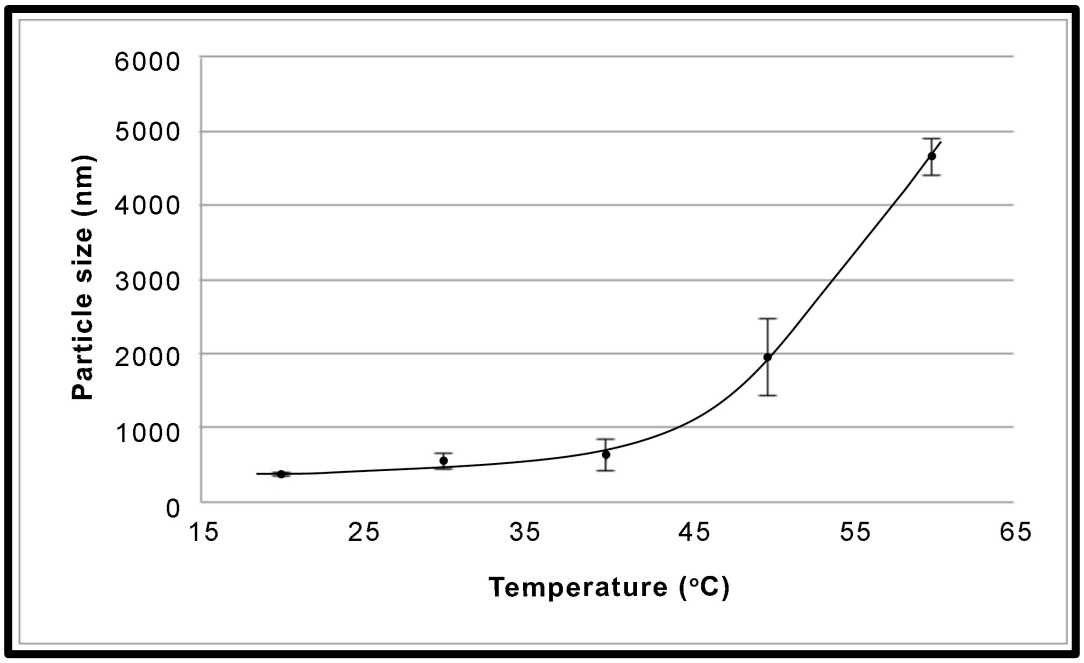

Figure 4.23. Variation of humate particle size with temperature in 40 mg/L LSLHA with 0.004 M $MgCl_2$ (pH 7.5).

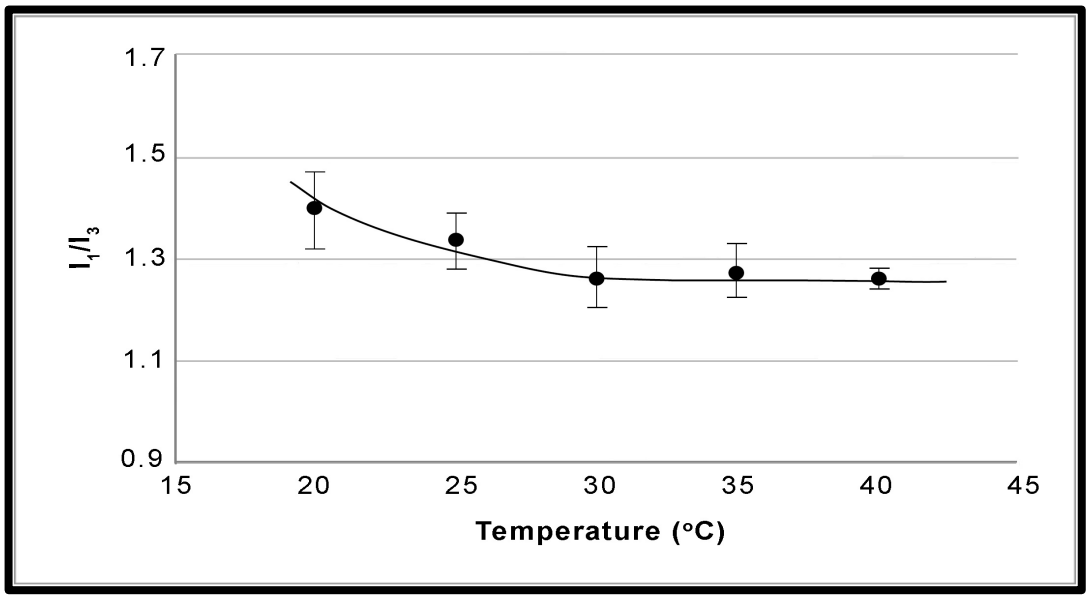

Figure 4.24. Variation of pyrene I_1/I_3 ratio with temperature in 40 mg/L LSLHA with 0.004 M $MgCl_2$ (pH 7.5).

The decrease of the pyrene I_1/I_3 ratio from 1.39 to 1.27 in the 20-40^{o} C range (Fig. 4.6) suggests that the probe became more sequestered in the humic environment in the presence of Mg^{2+} as the temperature was raised. The amount of aggregation beyond this temperature resulted in light scattering that interfered with the pyrene fluorescent measurements. However, the dynamic light scattering measurements indicated a change in particle size from 350 nm at 20^{o} C to 4650 nm at 60^{o} C.

Priming HA solutions for TIA/TIC by adding Mg^{2+} ions likely involved intra- and intermolecular crosslinking of the humic polymers and required an excess of the metal ion. The acid content of LSLHA was determined by a conductimetric method [15] and found to be 6.52 meq/g. When an equivalent amount of Mg^{2+} was added to LSLHA solutions, no TIC was observed at temperatures up to the boiling point. To assess the quantity of Mg^{2+} required to prime an aqueous LSLHA solution for TIC at 60° C, 3 µL aliquots of a 1.0 M $MgCl_2$ solution were slowly added to 25.0 mL of a 40 mg/L LSLHA solution held at this temperature. It was found that it required an approximately 14-fold excess of Mg^{2+} for visible clouding to occur. As noted above, an equivalent excess of positive charge provided by Na^{+} ions did not lead to clouding, confirming that electrostatic shielding alone is not sufficient for TIC. Similar results were obtained with $CaCl_2$. It appears that temperature induced effects caused by the addition of divalent cations were due to a combination of shielding and crosslinking.

4.4.4 Kinetic Effects

Aqueous humates in solutions of moderate ionic strength tend to precipitate

when left at room temperature for extended periods. Fig. 4.7 shows the development of particle size with time in a LSLHA/$MgCl_2$ solution at 30° C. It can be seen that a gradual particle growth process took place; after about 90 min precipitation began. The progression of the coagulation was highly temperature dependent: at 40° C precipitation started after 26 min; at 50° C it took 13 min; and at 60° C it took 6.5 min.

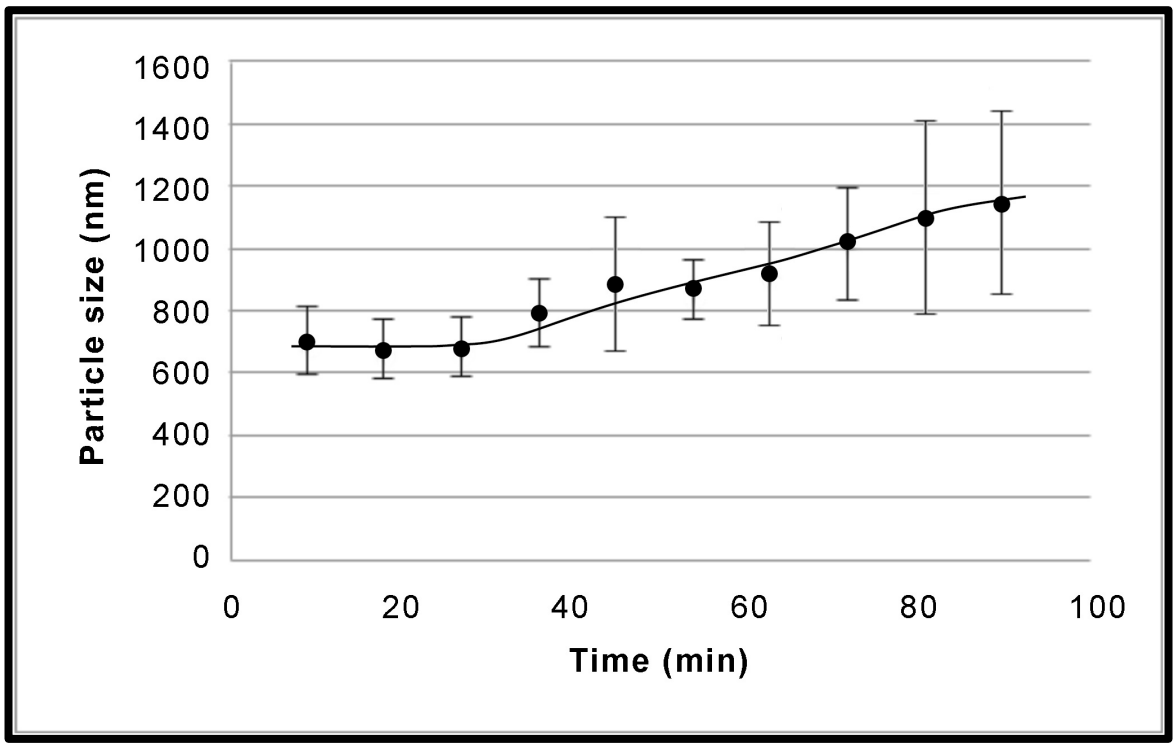

Figure 4.25. Time dependence of particle size in 40 mg/L LSLHA with 0.004 M $MgCl_2$ at 30° C (pH 7.5)

4.4.5. Declouding

When nonionic surfactants solutions are clouded by heating to the CP, complete resolubilization can be affected by cooling: TIC is an easily reversible process with these solutes, allowing for effective rehydration and dissolution by reverting to lower temper-

atures. Declouding of the humic suspensions studied here did not proceed effortlessly. Redissolution could be achieved by lowering the temperature, but it also required vigorous agitation. To examine this behavior, two identical 60 mg/L LSLHA solutions containing 0.004 M Mg^{2+} were clouded by heating to 60° C. One was kept at this temperature, and the other was cooled to 20° C, and both were vigorously shaken on a wrist-action shaker. Solutions were allowed to cool to room temperature, which took 45-60 min. Under this regimen, the solution at 60° C remained clouded, while the turbidity of the 20° C solution dissipated. Similar behavior was observed with LSLHA solutions that were clouded by lowering the pH to 2.5.

This declouding behavior can be rationalized by considering that temperature induced aggregation in humate solutions was initiated by dehydration, but the subsequent growth of the particles also involved entanglement and multiple interactions between the humic chains. At TIC, the particles responsible for the cloudy appearance were therefore held together by more than only hydrophobic interactions and could not be disrupted by merely increasing the dielectric constant of the aqueous solvent. Extensive agitation, together with a lower temperature, was needed to achieve redissolution.

4.5 Conclusion

The priming of humic solutions for temperature-induced effects requires judicious reduction of charge on the humate polymers. With electrostatic repulsion diminished, warming the solution leads to dehydration that promotes the growth of humic aggregates. In the absence of other interactions it is likely that this could be reversed by

simple cooling, but entanglement of the humic chains results in more durable particles that require mechanical disruption for complete redissolution.

4.6 References

[1] Šmejkalová D, Piccolo A. Aggregation And Disaggregation of Humic Supramolecular Assemblies by NMR Diffusion Ordered Spectroscopy (DOSY-NMR). Environ. Sci. Technol. 2008; 42(3):699–706.

[2] Wershaw RL. Molecular Aggregation of Humic Substances. Soil Sci. 1999; 164(11):803–813.

[3] Palmer NE, von Wandruszka R. Dynamic Light Scattering Measurements of Particle Size Development in Aqueous Humic Materials. Fres. J. Anal. Chem. 2001; 371(7):951–954.

[4] Malmberg CG, Maryott AA. Dielectric Constant of Water from 0^{o} to 100^{o} C. J. Res. Nat. Bur. Stand. 1956; 56(1):1–7.

[5] Engebretson RR, von Wandruszka R. Kinetic Aspects of Cation-Enhanced Aggregation in Aqueous Humic Acids. Environ. Sci. &Technol. 1998; 32(4):488–493.

[6] Product Literature, Coulter N4 Plus Sub micron Particle Sizer, Coulter Corporation, Miami, FL, USA.

[7] Ritchie JD, Perdue EM. Proton-Binding Study of Standard and Reference Fulvic Acids, Humic Acids, and Natural Organic Matter. Geochim. Cosmochim. Acta. 2003; 67(1): 85–96.

[8] Young C, von Wandruszka R. A comparison of aggregation behavior in aqueous humic acids. Geochem. Trans. 2001; 2–5:16–20.

[9] Dong D, Winnik M. The py Scale of Solvent Polarities. Solvent Effects on the Vibronic

Fine Structure of Pyrene Fluorescence and Empirical Correlations with E% and Y Values. Photochem. Photobiol. 1982; 35(1):17–21.

[10] Engebretson RR, von Wandruszka R. The effect of Molecular Size on Humic Acid Associations. Org. Geochem. 1997; 26(11-12):759–767.

[11] Basu Ray G, Chakraborty I, Moulik SP. Pyrene Absorption can be a Convenient Method for Probing Critical Micellar Concentration (CMC) and Indexing Micellar Polarity. J. Colloid Interface Sci. 2006; 94(1):248–254.

[12] Robinson RA, Stokes RH. Electrolyte Solutions, chapter 4, David & Charles, Newton Abbot, UK, 2nd edition, 2002.

[13] Drastík M, Novák F, Kučerík J. Origin of Heat-Induced Structural Changes in Dissolved Organic Matter. Chemosphere. 2013; 90 (2):789–795.

[14] Engebretson RR, von Wandruszka R. Micro-organization in Dissolved Humic Acids, Environ. Sci. Technol. 1994; 28:19-34.

[15] Riggle J, von Wandruszka R. Conductometric Characterization of Dissolved Humic Materials. Talanta. 2002; 57(3):519–526.

Chapter Five

A Kinetic and Thermodynamic Study of the Sorption of Perfluorinated Surfactants on Humic Materials

5.1 Abstract

Perfluorinated surfactants have become an environmental concern because of their potential toxicity. In view of the ubiquitous presence of humic substances in soils and natural waters, their sorptive interactions with perfluorooctane sulfonic acid (PFOS) and perfluorooctanoic acid (PFOA) were investigated in regard to the sorption kinetics and thermodynamics. An 80% crude blend Leonardite Humic Acid (CBLHA) and a local silt loam soil found in Latah County (LSL) were investigated to establish the absorption behaviors of these materials. The kinetic data were collected over a period of 84 h to ascertain that equilibrium conditions were attained. Sorption kinetics varied greatly with pH for CBLHA, and somewhat less so for LSL. This was due to the differences in electro-static interaction between the PFS adsorbates and the CBLHA and LSL adsorbents. Two kinetic models were considered for the sorption processes: the pseudo-second order model and the intra-particle diffusion model. Neither gave a perfect fit, but the pseudo-second order model provided the best agreement with the kinetic data. Two isotherm models were also applied to the sorption process: the Langmuir and Freundlich models. The Langmuir equation was found to provide a better fit than the Freundlich equation. Based on the sorption behaviors and the characteristics of the adsorbents and adsorb-ates, electrostatic interactions were determined to be the driving force in the sorption process between PFS and CBLHA and LSL.

5.2. **Introduction**

Perfluorinated compounds (PFCs) are man-made organic pollutants that have gained worldwide attention due to their ubiquitous global distribution and because they have been found in the blood samples of humans [1]. PFCs are extremely stable, causing them to be environmentally persistent and bioaccumulate in organisms [2,3]. These compounds have been used for many years in production of various household items. The most commonly recognized PFCs that are found in the environment are perfluorooctanoic acid (PFOA), which is used in the production of Teflon^{TM} products, and perfluorooctane sulfonic acid (PFOS), which is a breakdown product of chemicals that were formerly used in the production of Scotchgard products [4-6].

PFOS and PFOA are also key components of flame-retardant foams [7] that are used in fighting wildfires. PFOS and PFOA have a high degree of water solubility, which allows them to find their way into water bodies, including wastewater, surface water, ground water, and even drinking water [8-14]. They have been detected in these matrices all over the world [15].

The stability of PFSs makes it unlikely they will degrade in the environment [16]. Technology is available for the removal of PFOS and PFOA from aqueous environments. Reverse osmosis, nanofiltration membranes, and coagulation [17] have been used to remove PFOS from wastewater [18,19]; the sorption kinetics of PFOS and PFOA onto activated carbon and resin materials [20,21] have also been investigated. An aluminum coagulation method involving both slow and fast mixing to promote contact between the PFS and alumina has also been examined to remove PFSs from water [17].

These techniques have varying levels of effectiveness, but all require the introduction of additional xenobiotics into the environment. The use of humic material as an adsorbent would offer a naturally occurring alternative for the adsorption of PFCs in aqueous solutions. The objective of this study is, therefore, to thoroughly examine the sorption behaviors of PFOS and PFOA on an 80% CBLHA (a commercially available product) and LSLHA. ^{19}F NMR was used to examine the sorption kinetics and isotherms for PFOS and PFOA at different pH values with an eye on possible interactions that may lead to adsorption.

5.3. Materials and Methods

5.3.1 Materials

Potassium Perfluorooctane Sulfonate, 98% (PFOS, potassium salt) was purchased from Matrix Scientific and Perfluorooctanoic Acid, 95% (PFOA) was obtained from Alfa Aesar. Perfluorooctane amine was synthesized as described below. The physical properties of these compounds are detailed in Table 1.

Studies were performed with a crude leonardite humic acid (CBLHA), obtained under the trade name Agri-Plus from Horizon Ag-Products (Kennewick, WA) [22]. This is a mined material, subjected to minimal milling, and was used as received. It is a dark brown powder, with particle diameters in the 0.1-0.6 mm range and a density of 0.78 g/cm^3. It was reported by the purveyor to contain 80% humic acid, 5% fulvic acid, 15% clay, shale, gypsum, silica, and fossilized organic matter and to have a cation exchange capacity of 400-600 mequiv/100 mg [23]. The ash content was determined to be 13.37

± 0.05%. The carbon, hydrogen, and nitrogen contents, determined at the University of Idaho Analytical Sciences Laboratory, were 50.0, 4.9, and 1.1%, respectively. The metal content, determined according to the method reported by Pawluk [24], was found to be 140 µg/g Mg, 269 µg/g Ca, and 40 µg/g Cu. Pb, Sr, Cd, and Zn were not detected. In view of the crude nature of the material, variability between batches must be anticipated for all these parameters.

The top 30 cm of a Latahco silt loam soil (Argiaquic Xeric Argialbolls) maintained as pasture for at least 20 years, was collected, air-dried, and crushed to pass a 2.0 mm sieve. The collected soil contained 41.5 g organic C, 159 g clay, 121 g silt, and 3.9 g total N per kg soil. Organic carbon content was determined by the Walter-Black method, and total nitrogen by combustion (LEGO CHN-600 Determinator). Humic acid extraction was carried out according to the International Humic Substances Society (IHSS) procedure published on January 25, 1985. Of the Latahco silt loam humic acid (LSLHA) extracted, approximately one-half was deashed (DLSLHA) by the IHSS method, while the other half was left untreated (NLSLHA). NLSLHA and DLSLHA contained 24.0% and 1.8% ash, respectively, on a moisture free basis. The metal content of the above humic acids was measured by ICP spectrometry (Leman Labs Model PS 3000) by the Analytical Services Laboratory at the University of Idaho, following standard procedures for soils.

5.3.2 Sorption Kinetic Experiments

Eight different suspensions were created to determine the conditions for maximum adsorption of PFS onto CBLHA. Each vial contained 20.0 mL of 0.002M PFS and a different mass of the humate: the vial with the least contained 0.5g CBLHA and it went

up by 0.5 g in each vial, with the last one holding 4.0g of adsorbent. The solutions were the placed on a Burrell Wrist Action Shaker for 48 h and then filtered using a glass wool filter pipette. The PFS remaining in the filtrate was determined using ^{19}F NMR spectroscopy. Fig 5.1 shows an example of the of ^{19}F NMR spectra that was used to determine the isotherm of PFOA on the CBLHA. The standard material was an aqueous solution of 0.002M PFOA. This is also the concentration used for the kinetics experiments for both PFOS and PFOA. The spectrum for the standard material gave a relatively large triplet at approximately -81.4ppm, representing the terminal CF_3 on the PFOA/PFOS carbon chain. This peak of the standard material was integrated for a set number of scans and then equated to 100%. The next spectra were run for the same number of scans, integrated, and then compared to the standard material to give a percentage of PFOA/PFOS that was left in solution. This percentage was then used to determine the amount of PFS adsorbed. The kinetics experiments were different only to the extent that time, rather than she solute concentration, was varied. The maximum adsorption (i.e. minimal amount of F left in the filtrate) was observed in the sample containing 1.5 g CBLHA. This mass was used throughout the kinetics experiments.

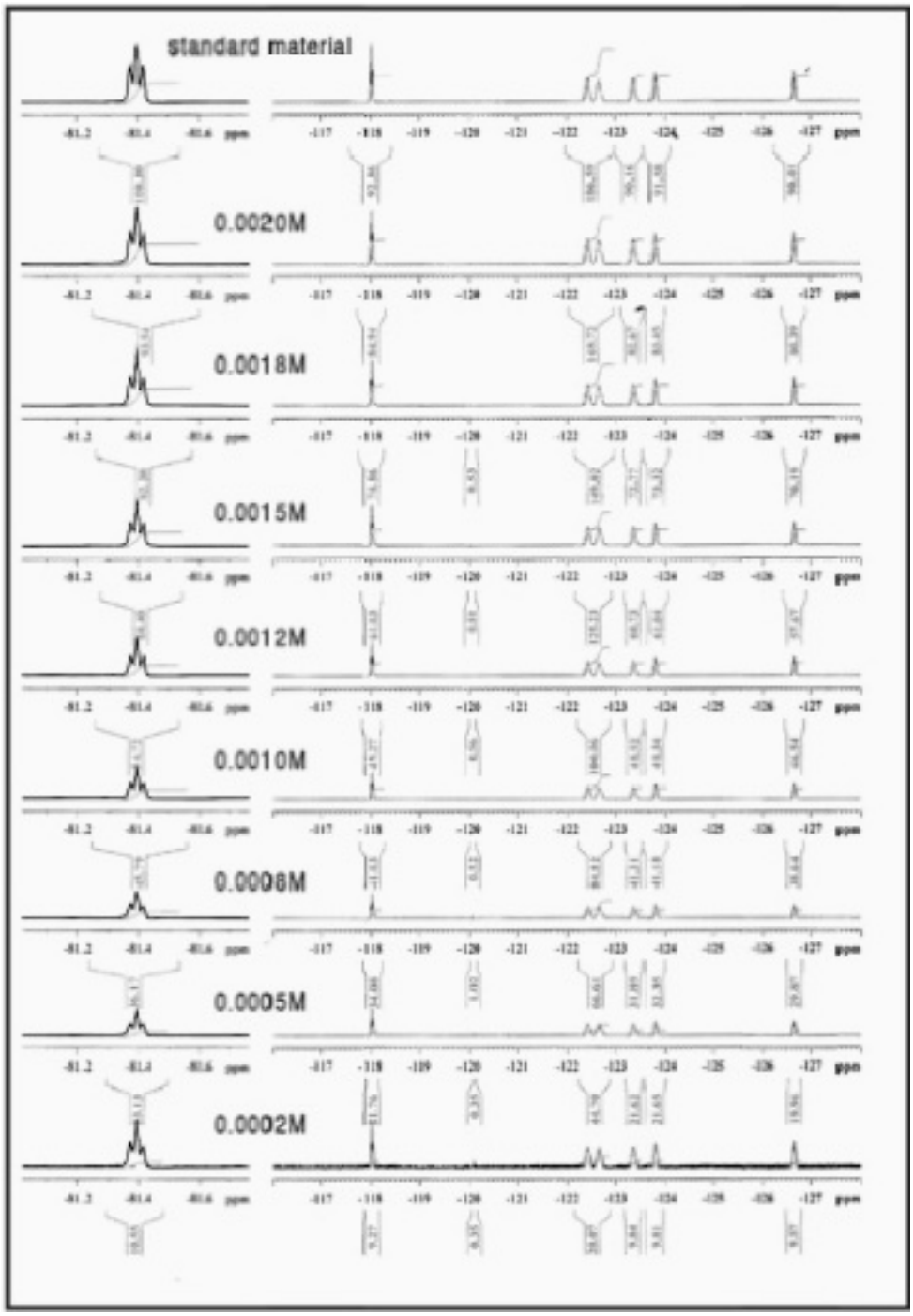

Figure 5.1 ^{19}F NMR spectra of PFOA on 0.250 g of CBLHA at pH 5. The triplet at -81.4 ppm was used for quantitation. Concentrations of PFOA are indicated on spectra.

As noted above, the kinetics experiments were performed by adding 1.5 g of the humic material and 20 mL of 0.002M perfluorinated surfactant. Eight solutions were placed on

the Burrell wrist action shaker and one solution was removed every 12 hours with the longest one running 96 hours.

All kinetic and isotherm studies were carried out at pH values of 2, 5, and 7. The pH was adjusted by adding concentrated hydrochloric acid or aqueous ammonia. Humic materials naturally buffer solutions at a pH around 5. The pH of the CBLHA solutions naturally adjusted itself to this value, so no adjustment was necessary for pH 5 solutions. When NH_4OH was used to adjust the pH of the humic suspension to 7, a little dissolution did occur. Eventually the pH drifted down to 5 again in these solutions.

5.3.3 Sorption Isotherm Experiments

The solutions for the isotherm study were prepared in a similar fashion. In this case, however, the PFS concentration of the solution was the variable and the mass of the humic adsorbent was constant, as was the time of contact. In order to insure that all the adsorption sites on the CBLHA were filled, 0.25 g of the humate was used and the concentrations of the PFS adsorbate varied from 0.0002M to 0.002M.

Table 5.1. Physiochemical properties of PFOS and PFOA.

Compound	Molecular Formula	Molecular Weight	Molecular Volume	Water Solubility	pKa
PFOS	**$C_8F_{17}SO_3K$**	**538.23**	**257**	**570mg/L**	**-3.27**
PFOA	**$C_7F_{15}COOH$**	**414.07**	**226**	**9.5×10^3mg/L**	**2.8**

5.3.4 PFOS and PFOA Determination

After exposure of the adsorbent and adsorbate in the sorption experiments, the mixtures were filtered using a glass-wool pipette, Fig 1, followed by filtration through a 0.22 µm nylon membrane. Control experiments showed negligible loss of PFS on the filter media. Due to the light absorption and surfactant properties of humic materials, detection of PFSs humate solutions by optical spectroscopy or chromatography can be challenging. It was found that the concentrations of PFSs were best determined by ^{19}F NMR. A deuterium source was needed for the NMR deuterium lock. Deuterated DMSO was added to an NMR tube insert that was placed in the NMR tubes containing the aqueous solutions. The sorption quantity was calculated by comparing the PFS concentrations in solution before and after the sorption process.

Figure 5.2. Glass-wool filter pipette

5.4. Results and Discussion

5.4.1 Sorption Kinetics

Although humic materials are technically zwitterionic [25] the humic chains are rich in carboxylic moieties, which give them an overall negative charge. The adsorbates PFOS and PFOA are functionalized with a sulfonate and a carboxylate group respectively, making them generally negative. Therefore, it can be predicted that changing the pH of

the solution would impact the repulsion between the adsorbent and the adsorbate. The kinetic profiles for the PFOS and the PFOA vary greatly at different pH values. It took a full 60 h to reach the sorption equilibrium for PFOS on CBLHA at a pH of 2. This humic material is granular and porous like activated carbon but is highly functionalized. At a lower pH the electrostatic repulsion was lower allowing the PFOS to "wriggle" inside of the humic aggregates. This resulted in a greater amount of adsorption, but the kinetics for the process was very slow. At a pH of 5 the repulsion was greater, allowing a smaller quantity of adsorbate to bind to the humic acid, and at a pH of 7, when the repulsion was at its maximum, none of the PFSs bound to the CBLHA.

The sorption kinetics curve, in which the quantity of PFS adsorbed (q_t) is plotted against time (in hours), is shown in Fig 5.3 and Fig 5.4. It is clear that the initial adsorption proceeded relatively rapidly, and then leveled off at a saturation value.

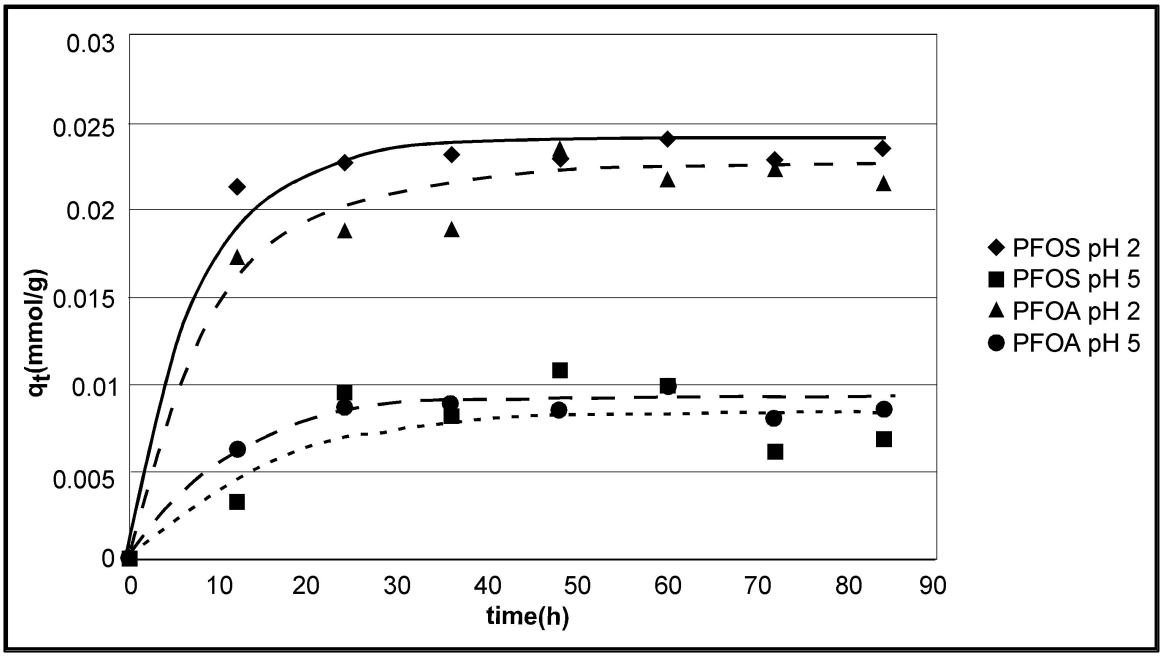

Figure 5.3. Sorption Kinetic of PFOS and PFOA on CBLHA.

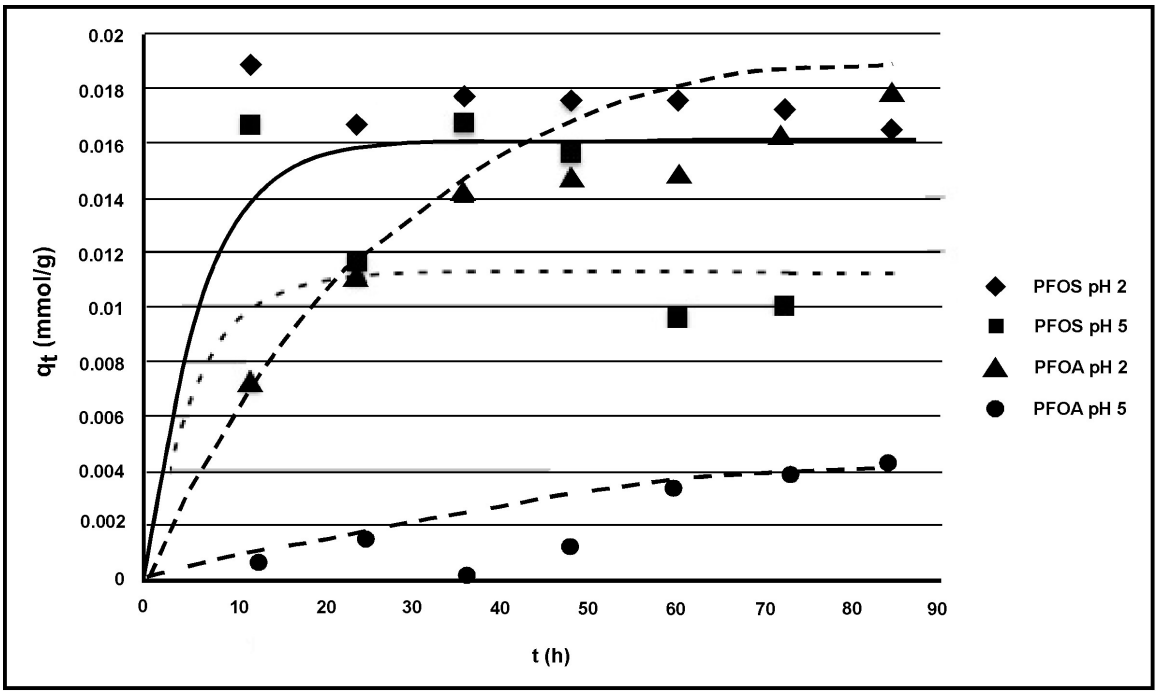

Figure 5.4 . Sorption Kinetic of PFOS and PFOA on CBLHA.

Adsorption processes of this kind have been modeled in different ways, two of which will be explored below.

5.4.1.1 Pseudo-second order rate model

A pseudo-second order kinetic model was selected to fit the data. This model assumes that the rate of sorption is controlled by chemical sorption, and the sorption capacity is a factor of the number of active sites that are available on the sorbent [26].

The equation [27]:

$$\frac{t}{q_t} = \frac{1}{k_2 q_e^2} + \frac{t}{q_e} = \frac{1}{v_0} + \frac{t}{q_e} \qquad [1]$$

where

q_e = equilibrium sorption capacity,

q_t = sorption capacity at time t,

k_2 = sorption rate constant,

$v_o = \kappa_2 q_e^2$ = initial sorption rate constant

mathematically represents the sorption process. When this kinetic model is applicable, the value of q_e does not have to be assigned *a priori* or estimated from the graph. Its value is obtained by plotting t/q_t against t, which is a linear relationship from which not only q_e, but also k and v_o can be determined (using the slope and intercept). Fig 5.5 shows these plots for various sorption scenarios with CBLHA. This plot and the data in Table 5.2 indicate that the pseudo-second order rate model for PFS sorption onto CBLHA and LSL was imperfect. Previous systems studied in this manner were somewhat heterogeneous, but far less so than the adsorbents considered here. For adsorption of PFOS/PFOA onto CBLHA, the q_e values determined followed a predictable trend, in so far that they were much smaller at pH 5 than at pH 2. At the higher pH, the mutual electrostatic repulsion between the acidic surfactants and the partially dissociated carboxylates of the humate in CBLHA inhibited the approach of the two species. At pH 2, on the other hand, many of the acidic moieties were protonated and sorption could proceed more vigorously.

The values of k_2 (and hence the related values of v_o), varied widely and unpredictably for PFS/CBLHA. With PFOS at pH 5, k_2 even became negative, which is physically meaningless. For this system it was also found that the correlation coefficient (R^2) was low, leading to the conclusion that the model failed here. A possible cause of this was that while the intercepts of the curves in Fig. 5.5 were necessarily close to zero, in situations of high statistical scatter, the fitted line could readily produce a negative intercept.

The heterogeneity of the adsorbent was also a possible cause of this failure, as different sorption mechanisms were at work at the same time. In view of this, all values of k_2 should be regarded with a degree of caution.

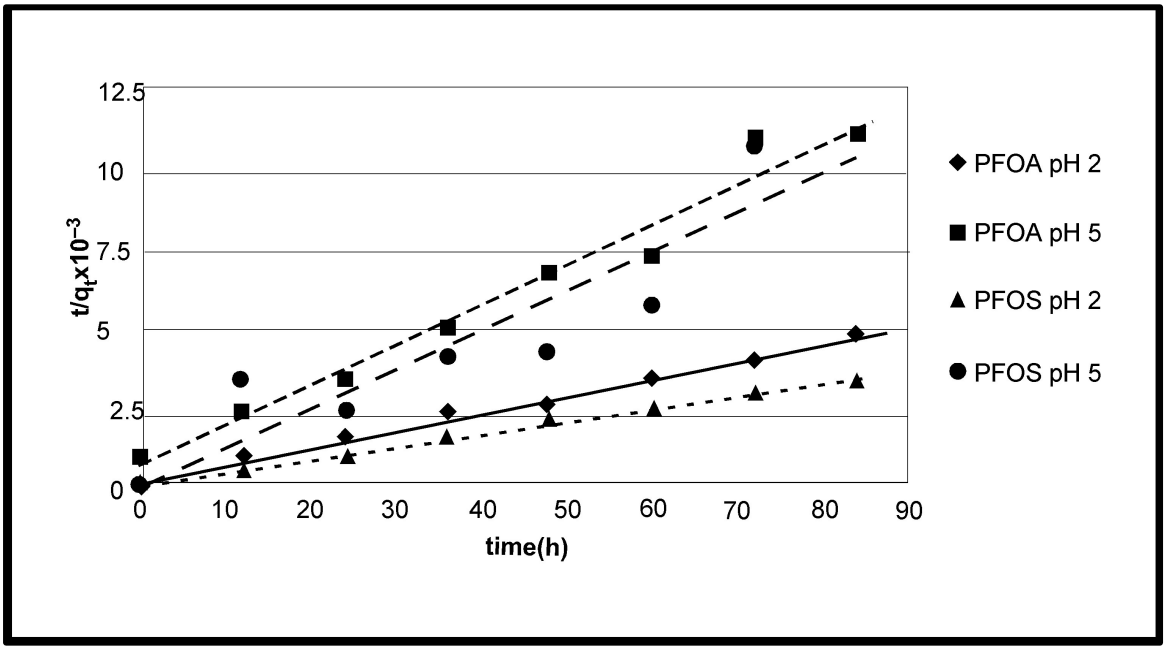

Figure 5.5. Kinetic data for the sorption of PFOS and PFOA to CBLHA at pH values of 2 and 5.

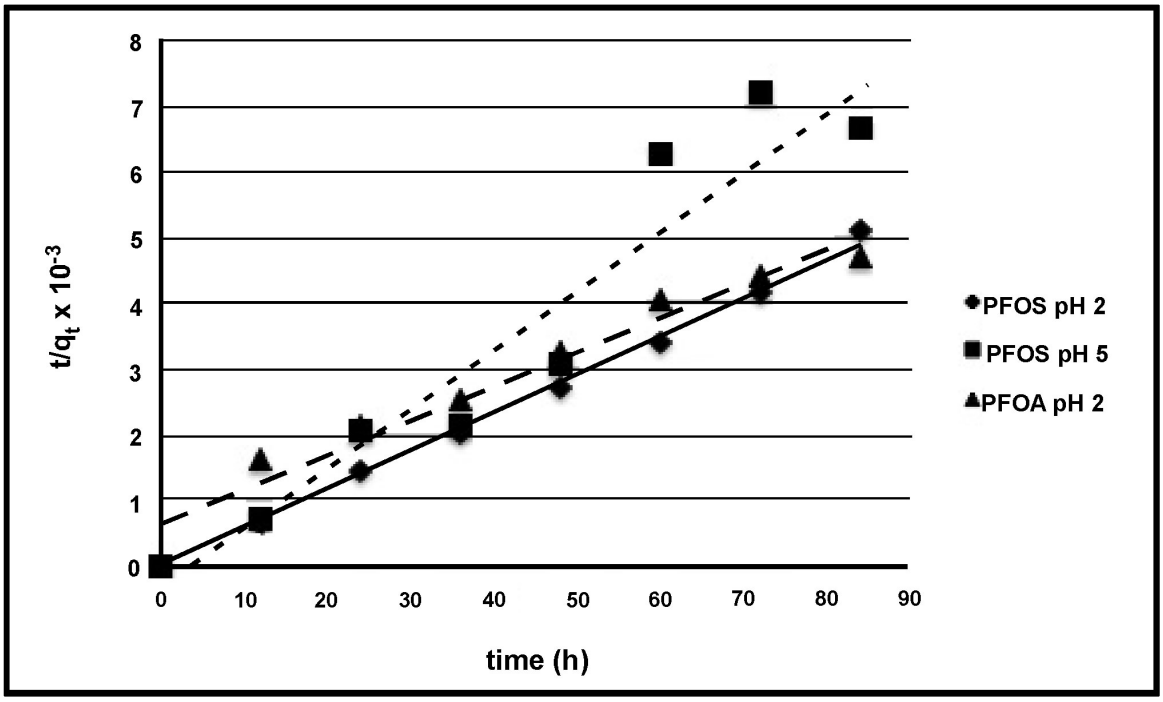

Figure 5.6. Kinetic data for the sorption of PFOS and PFOA to LSL at pH values of 2 and 5.

In regard to heterogeneity and the likelihood of multiple PFS adsorption mechanisms, the situation with LSL was even more distinct than that with CBLHA. This soil has a relatively high organic carbon content of 12.9%, the remainder being clay and silt. Adsorption on such a medium clearly proceeded in a variety of ways, which is borne out by the kinetic parameters shown in Table 5.2. Even for PFOS at pH 2, the k_2 measurements did not provide consistent results (Fig 5.6).

Table 5.2 Kinetic parameters of the pseudo-second order model for PFOS and PFOA

Adsorbent	Adsorbate	pH	q_e	v_o	k_2	k_d	D	R^2
CBLHA	PFOS	2	0.024	0.034	61.51	0.0049	0.916	0.999
		5	0.0074	-0.014	-261.1	0.0018	1.00	0.864
	PFOA	2	0.023	0.0083	16.13	0.0018	0.567	0.990
		5	0.0095	0.0021	23.42	0.0032	1.177	0.975
LSL	PFOS	2	0.016	-0.0029	-57.40	0.0038	-	0.997
		5	0.011	0.0029	24.75	0.0028	-	0.920
	PFOA	2	0.019	0.0016	4.429	0.0023	-	0.954
		5	0.006	0.0001	2.46	0.0004	-	0.206

5.4.1.2 Intra-particle diffusion model

The adsorption process can be divided into three steps [28], the first being the external diffusion phase where the adsorbate moves from the bulk solution to the external surface of the adsorbent. Next, in the intra-particle diffusion stage (commonly the rate-controlling step [29]) the adsorbate diffuses deeper into the adsorbent matrix. The final stage involves the actual adsorption of the adsorbate to the active site on the adsorbent.

The intra-particle diffusion model assumes that the external diffusion is negligible and intra-particle diffusion is the only rate-controlling step. In this model, the quantity of adsorbate adsorbed at time *t*, q_t, is related to the relevant parameters by the equation [30]:

$$q_t = \frac{6q_e}{r}\left(\frac{D}{\pi}\right)^{\frac{1}{2}} t^{\frac{1}{2}} = k_d t^{\frac{1}{2}} \qquad [2]$$

where:

k_d = intra-particle diffusion rate constant

r = particle radius

q_e = equilibrium sorption amount

D = intra-particle diffusivity

Figs. 5.7 and 5.8 show a series of plots of q_t *vs.* $t^{1/2}$, in accordance with equation [2], which was used to determine k_d, and hence D. The values of these two diffusion parameters are also shown in Table 2, albeit only for CBLHA. The reason that the LSL data were not used in this model was that this soil had many dissimilar components, comprising organic, clay, and silt materials, so that no reasonable estimate for the radius, r, could be extracted. For CBLHA, which primarily consists of humate, an estimated particle radius of 2.5 mm was used in the calculations. This estimate was based on the mesh size of the sieve used in the preparation of the material.

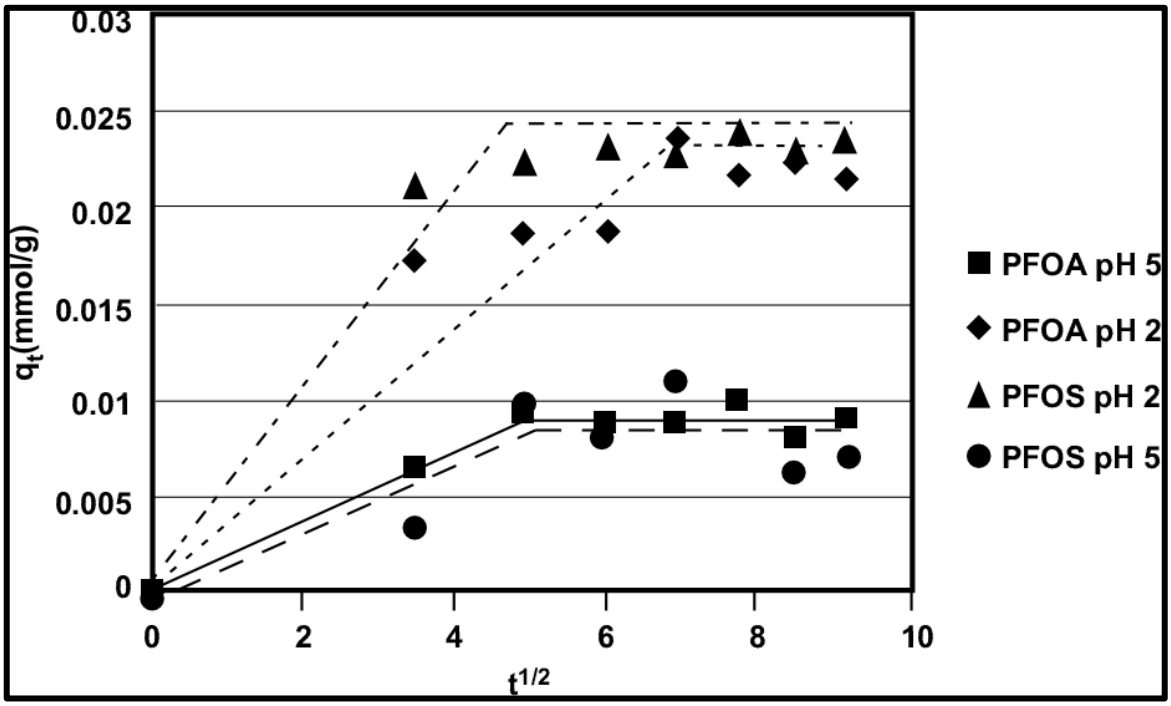

Figure 5.7. Intra-particle diffusion model for the sorption of PFOS and PFOA on CBLHA at a pH of 2 and 5.

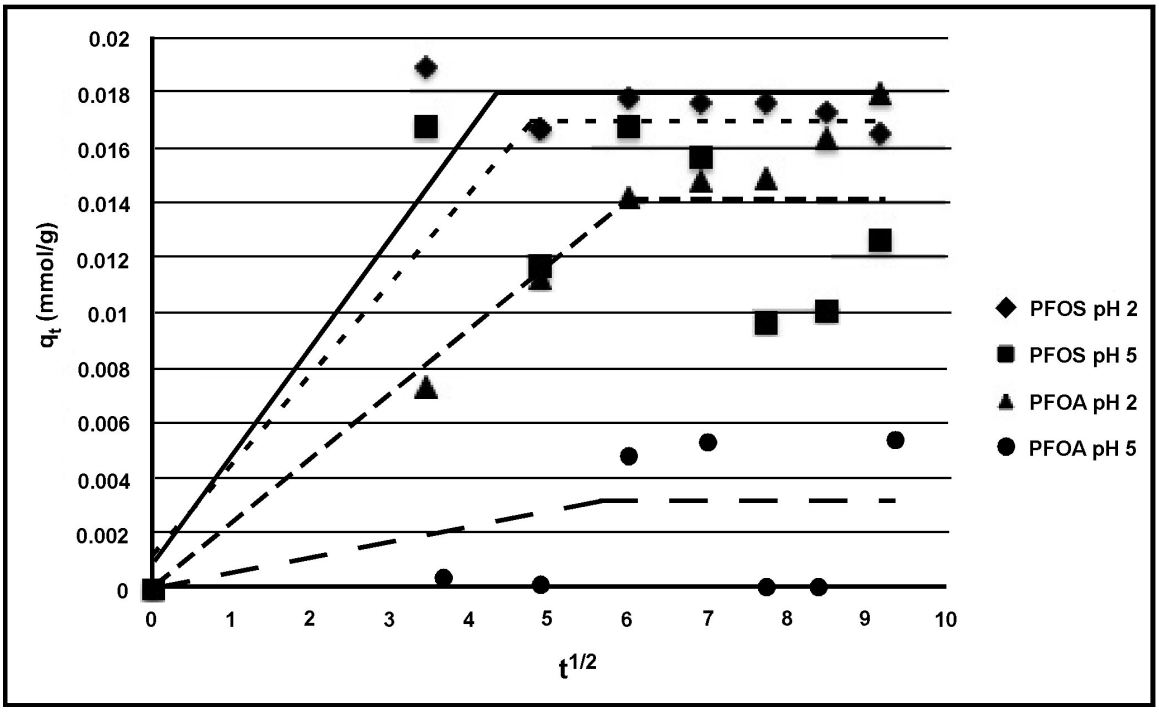

Figure 5.8 Intra-particle diffusion model for the sorption of PFOS and PFOA on LSL at a pH of 2 and 5.

As can be seen from the sorption capacity data in Table 5.2, there was a great deal of variability between the adsorbents, adsorbates, and environmental parameters. The PFOS and the PFOA gave differing results for the kinetic parameters with regard to their sorption on CBLHA. At low pH, PFOS adsorbed better to CBLHA than PFOA. The kinetic parameters for PFOS were significantly higher than those for PFOA at a pH of 2 and 5, with the exception of the equilibrium sorption capacity, which was almost the same for the PFOS and PFOA at a pH of 5. The diffusion coefficient for PFOS was also substantially higher than that of PFOA, which may be related to a greater degree of hydration of the latter. PFOS and PFOA both adsorbed significantly better at pH 2, which leads to the conclusion that the binding process between the adsorbate and the adsorbent was in-

deed due to electrostatic interactions. The maximum adsorption at pH 5 was significantly lower for both PFOS and PFOA. This is compatible with our reasoning because the pK_a of PFOA is approximately 2.8 and at pH 5 both PFOS and PFOA would be similarly negative and would experience similar repulsion from the carboxylic moieties on the humic chains on the adsorbent.

5.4.2 Sorption Isotherms

The Langmuir and Freundlich theories are the two predominant theories used to describe sorption processes in natural systems and to provide information regarding the chemical interactions between adsorbent and adsorbate. The two isotherms in question are mathematically expressed as follows:

Langmuir:

$$q_e = \frac{bq_mC_e}{1+bC_e} \qquad [2]$$

Linearized form: $$\frac{1}{q_e} = \frac{1}{q_m} + \frac{1}{q_m bC_e} \qquad [3]$$

Freundlich:

$$q_e = KC_e^{\frac{1}{n}} \qquad [4]$$

Linearized form: $$logq_e = logK + \frac{1}{n}logC_e \qquad [5]$$

where:

q_e = equilibrium sorption capacity

b = Langmuir constant (an equilibrium constant)

q_m = maximum sorption capacity

C_e = equilibrium concentration of adsorbate in solution

K = empirical constant

n = empirical constant

For the work below, the *b, q_m, K, and n* values were determined graphically from the linearized equations [3] and [5]. The Langmuir isotherm, which only allows mono-layer coverage, is more commonly encountered in systems involving humates. Fig. 5.9 demonstrates that the isothermal data collected from the sorption experiments on CBLHA aptly fit the Langmuir isotherm model. This indicates that the PFOS and PFOA formed a monolayer on the active sites of the CBLHA adsorbent.

The Freundlich isotherm is an empirical model that is usually used in heterogeneous surface energy systems. There are some parts of the curve that coincide more with the Freundlich curve, but the Langmuir curve and the experimental data level off towards the end of the isotherm data which signifies that the adsorbate is not adhering to the adsorbent in multiple layers. This is indicates that the Langmuir isotherm model more accurately describes the thermodynamic interaction of the PFS to CBLHA than the Freundlich isotherm model does.

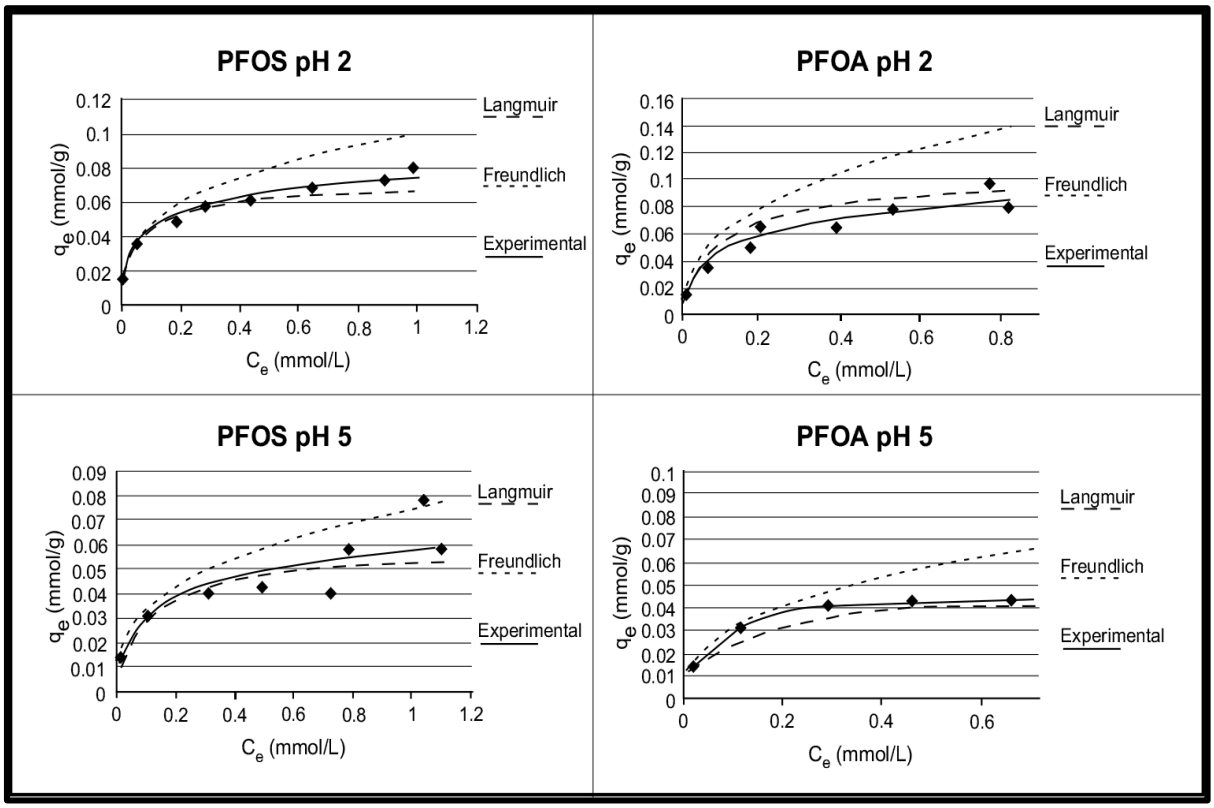

Figure 5.9. Isotherm data for PFOS and PFOA adsorbing on CBLHA at pH values of 2 and 5.

The isothermal and kinetic data of CBLHA and LSL, Fig. 5.10, were quite similar. The CBLHA had a much higher percentage of humic acid (80%), which gave a higher q_e for PFOS and PFOA at low pH, but lower sorption at a pH 5. The sorption kinetics for LSL were not as dependent on pH changes as those for CBLHA, but the LSL was not as effective an adsorbent as the CBLHA. In both instances the isotherms showed that the sorption reached a limiting value and then did not continue to adsorb more PFOS/PFOA indicating that it also follows the Langmuir isotherm.

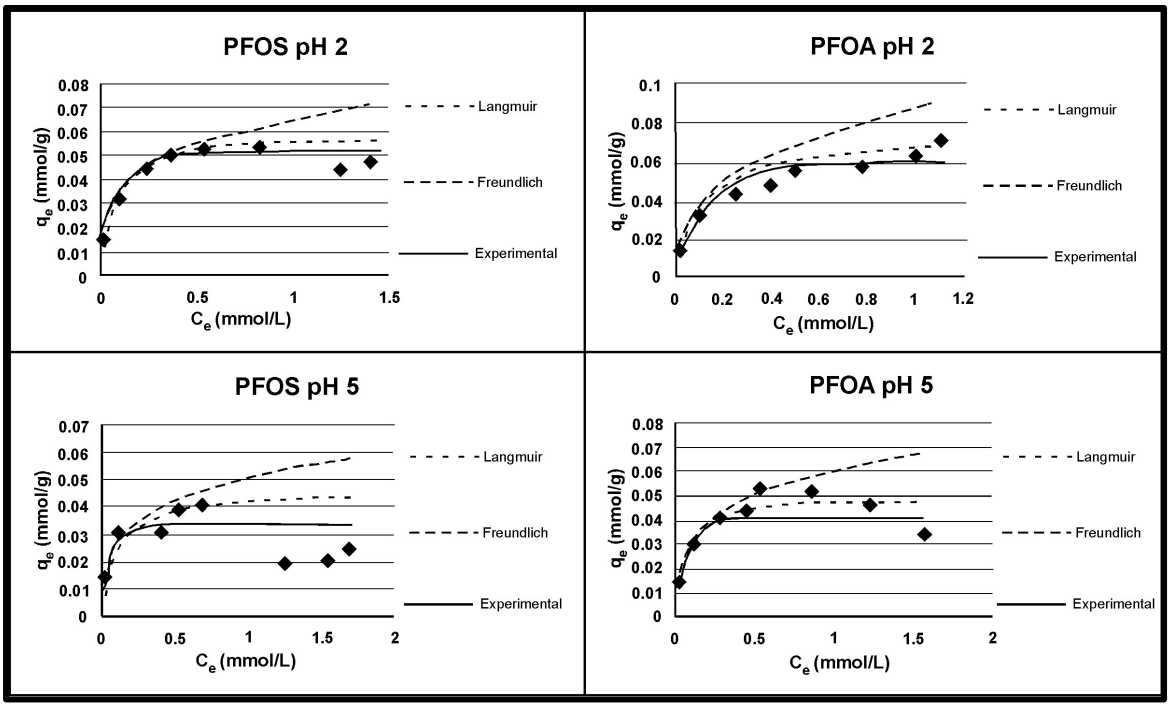

Figure 5.10 Isotherm data for PFOS and PFOA adsorbing on CBLHA at pH values of 2 and 5.

5.5. Conclusion

CBLHA was found to be a better adsorbent for PFOS and PFOA than LSL. LSL, however, was less susceptible to changes in solution parameters such as pH, indicating that the chemical (electrostatic) interactions between adsorbent and adsorbate were greater in the case of PFS adsorption to CBLHA than to LSL. The sorption kinetics for PFOA were slower than those for PFOS for both LSL and the CBLHA. PFOA reached equilibrium after 50 h on the CBLHA and after 36 h on LSL at pH 2. PFOS, however, reached equilibrium within 12 h at a pH 2 on both sorbents.

Out of the two models that were applied to the kinetic data, the pseudo-second order rate model gave the best fit, although it did not perfectly correspond to the data. This indicated that the interaction between the adsorbent and the adsorbates was pri-

marily due to chemical interactions. Both PFOS and PFOA fit the Langmuir model for the sorption isotherms on both LSL and CBLHA, indicating that the PFOS/PFOA adsorbed as monolayers.

5.5 References

[1] Eschauzier C, Beerendonk E, Scholte-Veenendaal P, de Voogt P. Impact of Treatment Processes on the Removal of Perfluoroalkyl Acids from Drinking Water Production Chain. Environmental Science and Technology. 2012; 57 (4): 631-638

[2] Giesy JP, Kannan K. Perfluorochemical Surfactants in the Environment. Environ. Sci. Technol. 2002; 36: 1681-1685.

[3] Loos R, Locoro G, Huber T, Wollgast J, Christoph EH, De Jager A, Gawlik BM, Hanke G, Umlauf G, Zaldivar JM. Analysis of Perfluorooctanoate (PFOA) and other Perfluorinated Compounds (PFCs) in the River Po Watershed in N-Italy. Chemosphere. 2008; 71: 306-313

[4] Janke A, Berger U. Trace Analysis of Per- and Polyfluorinated Alkyl Substances in Various Matrices- How do Current Methods Perform?. Journal of Chromatography A. 2009; 1216. (3): 410-421

[5] Post GB, Cohn PD, Cooper KR. Perfluoroctanoic Acid (PFOA), an Emerging Drinking Water Contaminant: A Critical Review of Recent Literature. Environmental Research. 2012; 116: 93-117

[6] Prevedouros K, Cousins IT, Buck RC, Korzeniowski SH. Sources, Fate and Transport of Perfluorocarboxylates. Environmental Science & Technology. 2006; 40 (1): 32-44

[7] Moody CA, Martin JW, Kwan WC, Muir DCG, Mabury SC. Monitoring perfluorinated surfactants in biota and surface water samples following an accidental release of fire-fighting foam into Etohicoke Creek. Environ. Sci. Technol. 2002; 36: 545-551

[8] Erickson I, Domingo JL, Nadal M, Bigas E, Lilebaria X, van Bavel B, Lindstrom G. Levels of Perfluorinated Chemicals in Municipal Drinking Water from Catalonia, Spain: Public Health Implications. Archives of Environmental Contamination and Toxicity. 2009; 57 (4): 631-638

[9] Hoffman K, Webster TF, Bartell SM, Weisskopf MG, Fletcher T, Viera VM. Private Drinking Water Wells as a Source of Exposure to Perfluorooctanoic Acid (PFOA)in Communities Surrounding fluoropolymer Production Facility. Environmental Health Perspectives. 2011; 119 (10): 92-97

[10] Jin YH, Liu W, Sato I, Nakayama SF, Sasaki K, Saito N, Tsuda S. PFOS and PFOA in Environmental and Tap Water in China. Chemosphere. 2009; 77 (5): 605-611

[11] Mak YL, Taniyasu S, Yeung LW, Lu G, Jin L, Yang Y, Lam PK, Kannan K, Yamashita N. Perfluorinated Compounds in Tap Water from China and Several Other Countries. Environmental Science & Technology. 2009; 43 (13): 4824-4829.

[12] Moody CA, Herbert GN, Strauss SH, Field JA. Occurrence and Persistence of Perfluorooctanesulfonate and Other Perfluorinated Surfactants in Groundwater at a Fire-Training Are at Wurtsmith Air Force Base, Michigan, USA. Journal of Environmental Monitoring. 2003; 5 (2): 341-345.

[13] Müller CE, Gerecke AC, Scheringer M, Hungerbuhler K. Identification of Perfluoroalkyl Acid Sources in Swiss Surface Waters with the Help of the Artificial Sweetner Acesulfame. Environmental Pollution Control Agency, St. Paul, Minnesota, USA. 2011.

[14] Murakami M, Imamura E, Shinohara H, Kiri K, Muramatsu Y, Harada A, Takada H. Occurrence and Sources of Perfluorinated Surfactants in Rivers in Japan. Environmental Science & Technology. 2008; 42 (17): 6566-6572

[15] Fuljii S, Polyprasert C, Tanaka S, Lien NHP, Qiu Y. New POPs in the water environment: distribution, bioaccumulation and treatment of perfluorinated compounds-a review paper. J. Water Supply Res. Technol. –Aqua. 2007; 56: 313-326

[16] Key BD, Howell RD, Criddle CS. Fluorinated Organics in the Bioshphere. Environ. Sci. Technol. 1997; 32: 2283-2287

[17] Xiao F, Simick MF, Gulliver JS. Mechanism for Removal of Perfluorooctane Sulfonate (PFOS) and Perfluorooctanoate (PFOA) from Drinking Water by Conventional and Enhanced Coagulation. Water Research. 2013; 47: 49-56

[18] Tang CYY, Fu QS, Robertson AP, Criddle CS, Leckie JO. Use of Reverse Osmosis Membranes to Remove Perfluorooctane Sulfonate (PFOS) from semiconductor Wastewater. Environ. Sci. Technol. 2006; 40: 7343-7349

[19] Tang CYY, Fu QS, Robertson AP, Criddle CS, Leckie JO. Effect of Flux (Transmembrane Pressure) and Membrane Properties on Fouling and Rejection of Reverse Osmosis and Nanofiltration Membranes Treating Perfluorooctane Sulfonate Containing Wastewater. Environ. Sci. Technol.206; 41: 2008-2014

[20] Yu Q, Zhang R, Deng S, Huang J, Yu G. Sorption of Perfluorooctane Sulfonate and Perfluorooctanoate on Activated Carbons and Resin: Kinetic and Isotherm Study. Water Research. 2009; 43: 1150-1158

[21] Yao Y, Volchek K, Brown CE, Robinson A, Obal T. Comparitive Study of Adsorption of Perfluorooctane Sulfonate (PFOS) and Perfluorooctanoate (PFOA) by Different Adosrbents in Water. Water Science and Technology. 2014; 70 (12): 1983-1991

[22] Yates LM III, von Wandruszka R. Decontamination of Polluted Water by Treatment with a Crude Humic Acid Blend. Environ. Sci. Technol. 1999; 33: 2076-2080

[23] *Product Guide: 1983:* Horizon Ag-Products, 2810 W. Clearwater, Kennewick, WA 99336. 1983

[24] Pawluk, S. *At. Absorpt. Newsl.* 1967; 6: 53.

[25] Eladia M, Peña-Mendez JH, Jirí P. Humic substances ñ compounds of still unknown structure: applications in agriculture, industry, environment, and biomedicine. J. Appl. Biomed. 2005; 3: 13-24

[26] Ho YS, McKay G. Pseudo-second order model for sorption processes. *Process Biochem*. 1999; 34: 451-465.

[27] Ho YS, McKay G. A Comparison of chemisorption kinetic models applied to pollutant removal on various sorbents. Process Saf. Environ. Protect. 1998; 76: 332-340.

[28] Chingombe P, Saha B, Wakeman RJ. Sorption of Atrazine on Conventional and Surface Modified Activated Carbons. J. Colloid Interface Sci. 2006; 302: 408-416

[29] Yang X, Al-Duri B. Kinetic Modeling of Liquid-Phase Adsorption of Reactive Dyes on Activated Carbon. J. Colloidal Interface Sci. 2005; 287: 25-34

[30] Boyd GE, Adamson AW, Myers Jr. LS. The exchange adsorption of ions from aqueous solutions by organic zeolites. II. Kinetics. J. Am. Chem. Soc. 1947; 69: 2836–2848.